廣西大學
GUANGXI UNIVERSITY

MicroPattern Gaseous Detectors (GMCP & THGEM) for Particle Detection in Space

Hongbang Liu
Guangxi University

On behalf of CXPD, POLAR-2/LPD and HERD/TRD Calibration

Contents

廣西大學
GUANGXI UNIVERSITY

Introduction

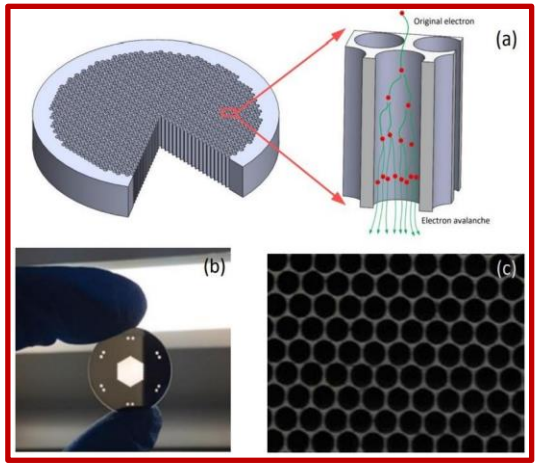

Gaseous Microchannel Plate (GMCP)

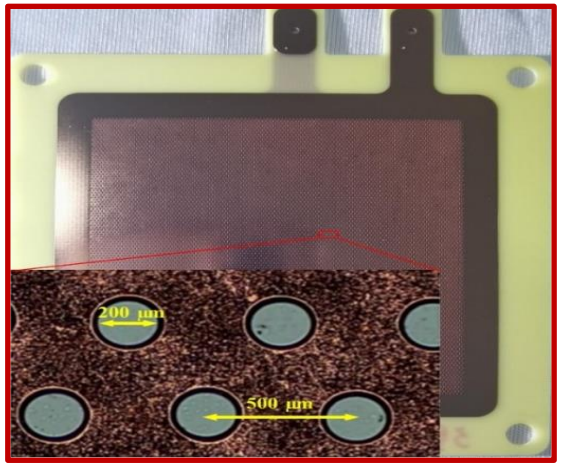

THick Gaseous Electron Multiplier (THGEM)

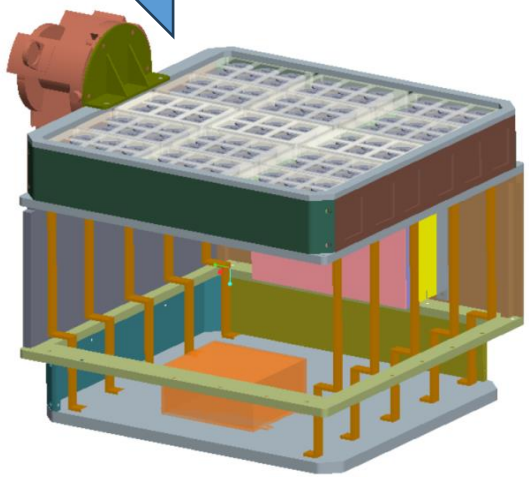

POLAR-2/LPD

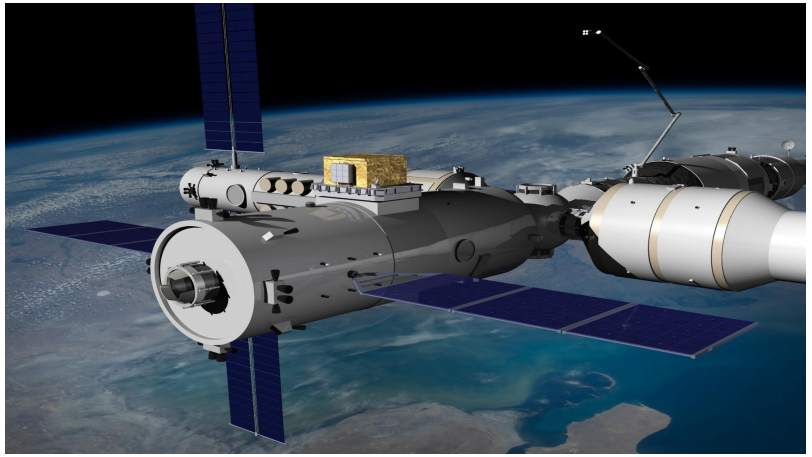

China Space Station

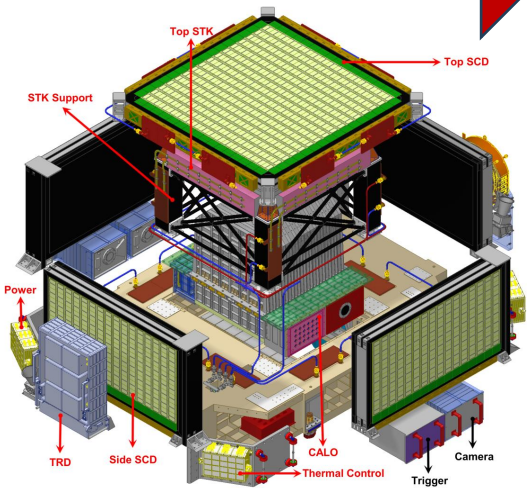

HERD/TRD

Scientific goals of POLAR-2/LPD

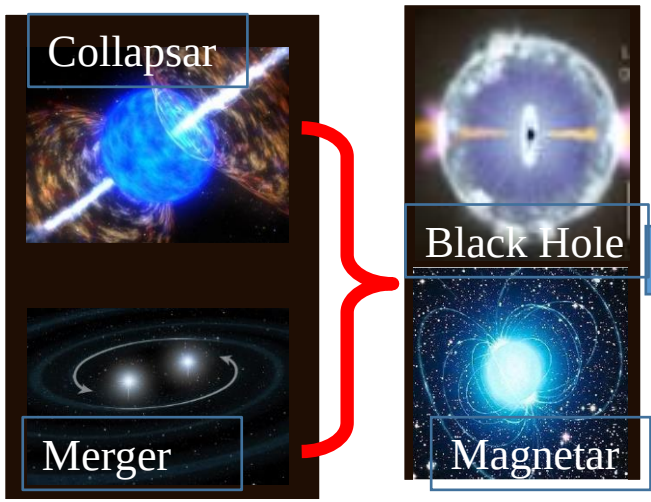

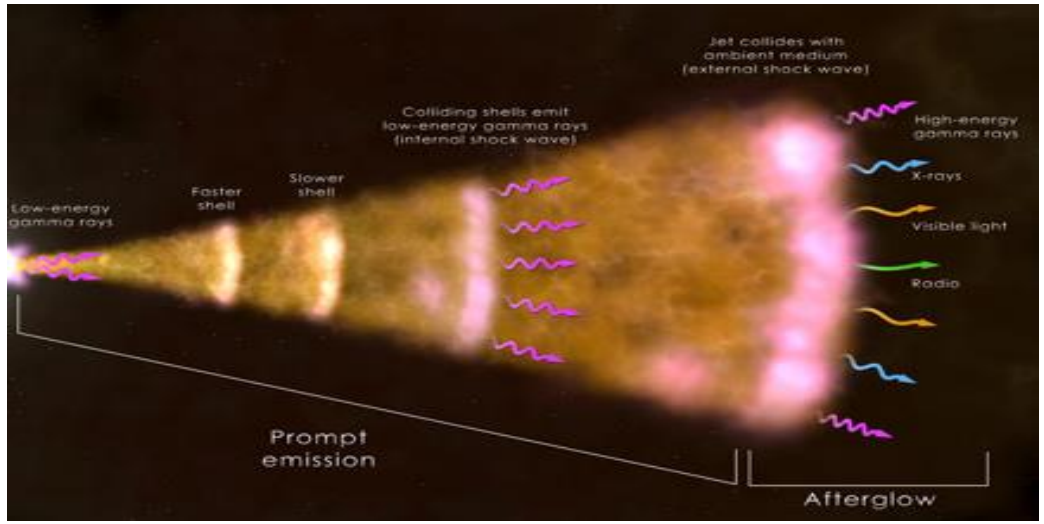

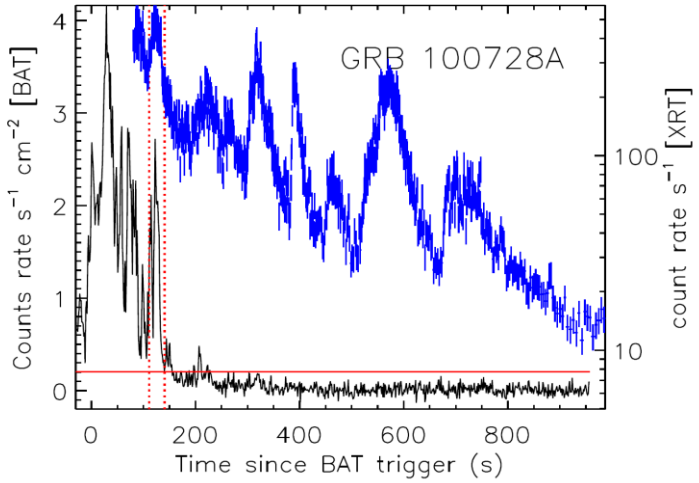

Gamma-ray bursts

- massive stars explosions
- neutron stars or black holes mergers

Are gamma-ray bursts and X-ray flares of the same origin?

What is the GRB radiation mechanism?

Scientific requirement

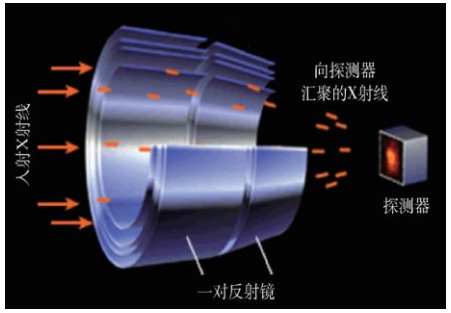

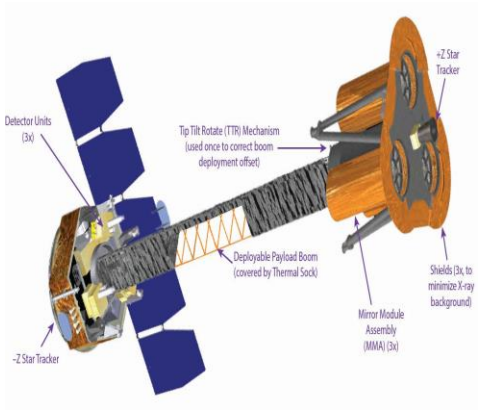

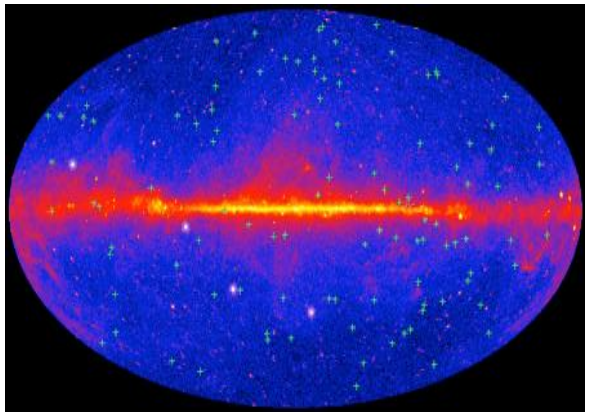

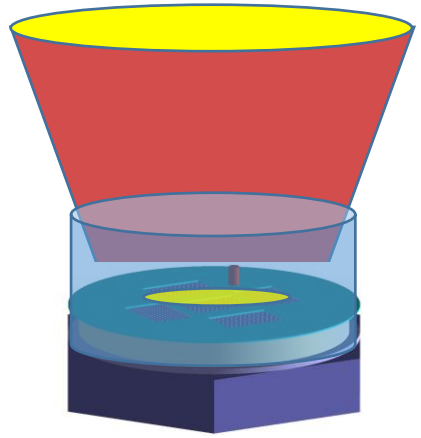

- IXPE: grazing incidence telescope, narrow field of view
- Objects: Bright X-ray sources, such as Crab, Vela, pulsars, etc.

- GRBs are transient sources that appear unpredictably, without prior knowledge of when or where they will occur.
- Requires LPD with large area and wide field of view

Polar2/LPD payload and detection principle

➢Polar-2/LPD payload

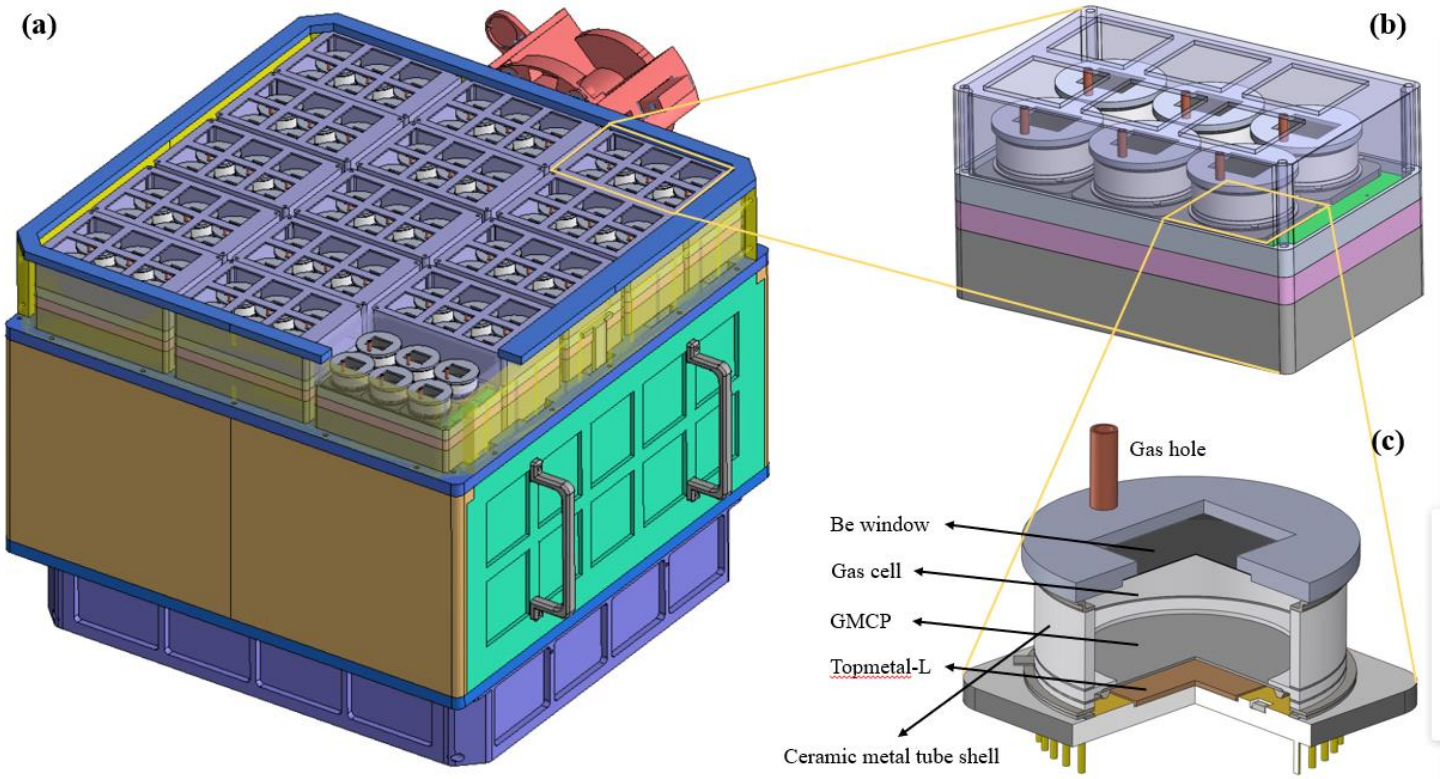

➢Principle of polarization detection

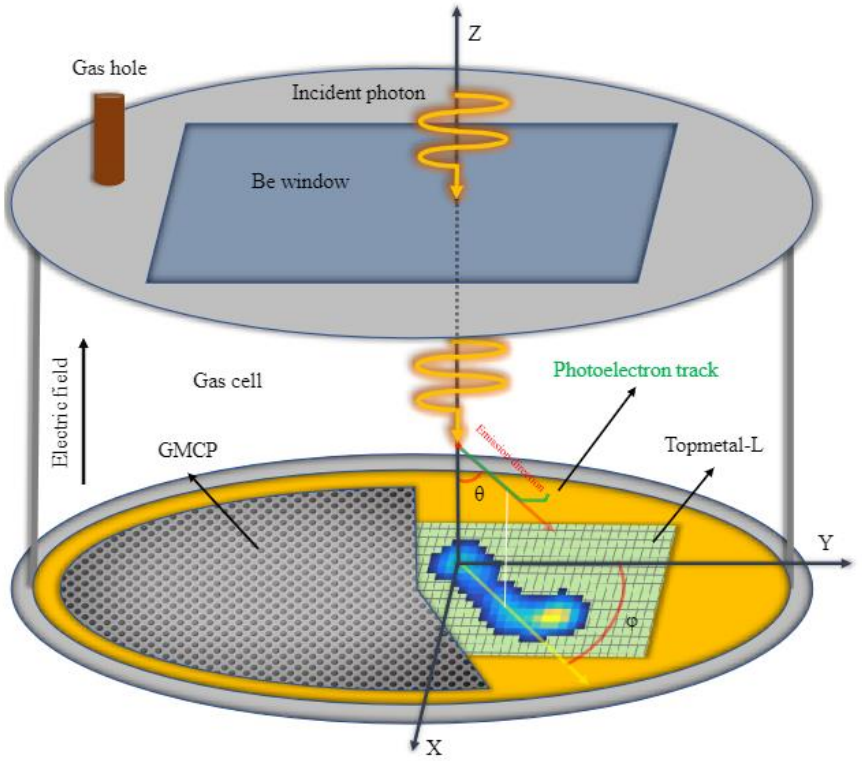

LPD in orbit simulation

廣西大學 GUANGXI UNIVERSITY

➢Chinese space station orbit

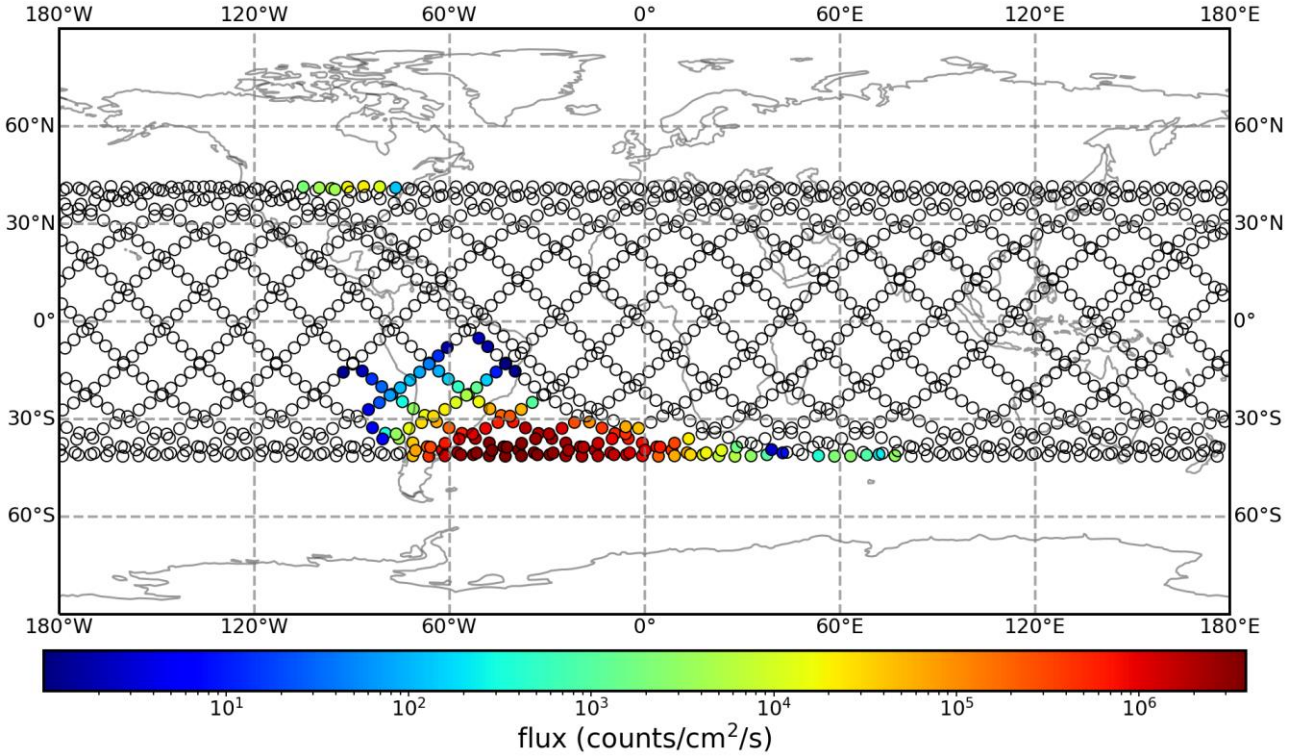

The projection of LPD orbit on Earth in 1 day

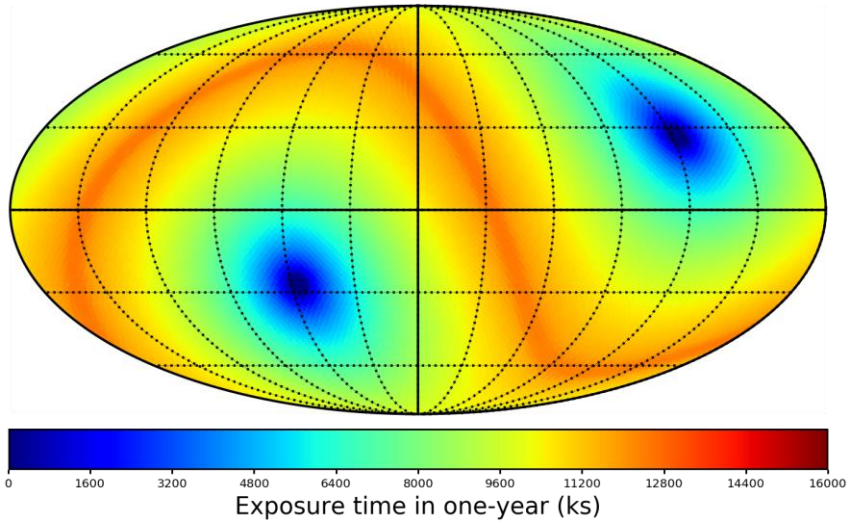

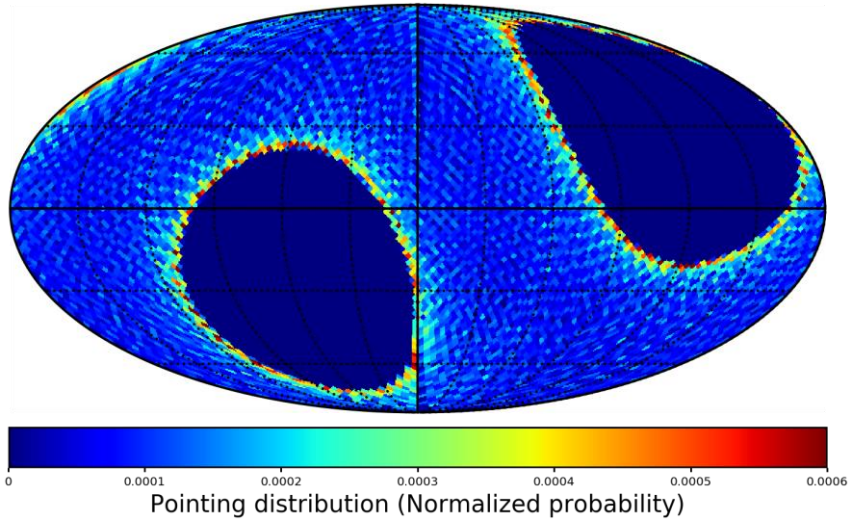

Polarization Statistics

➢ Statistical distribution of MDP of LPD in 5 years

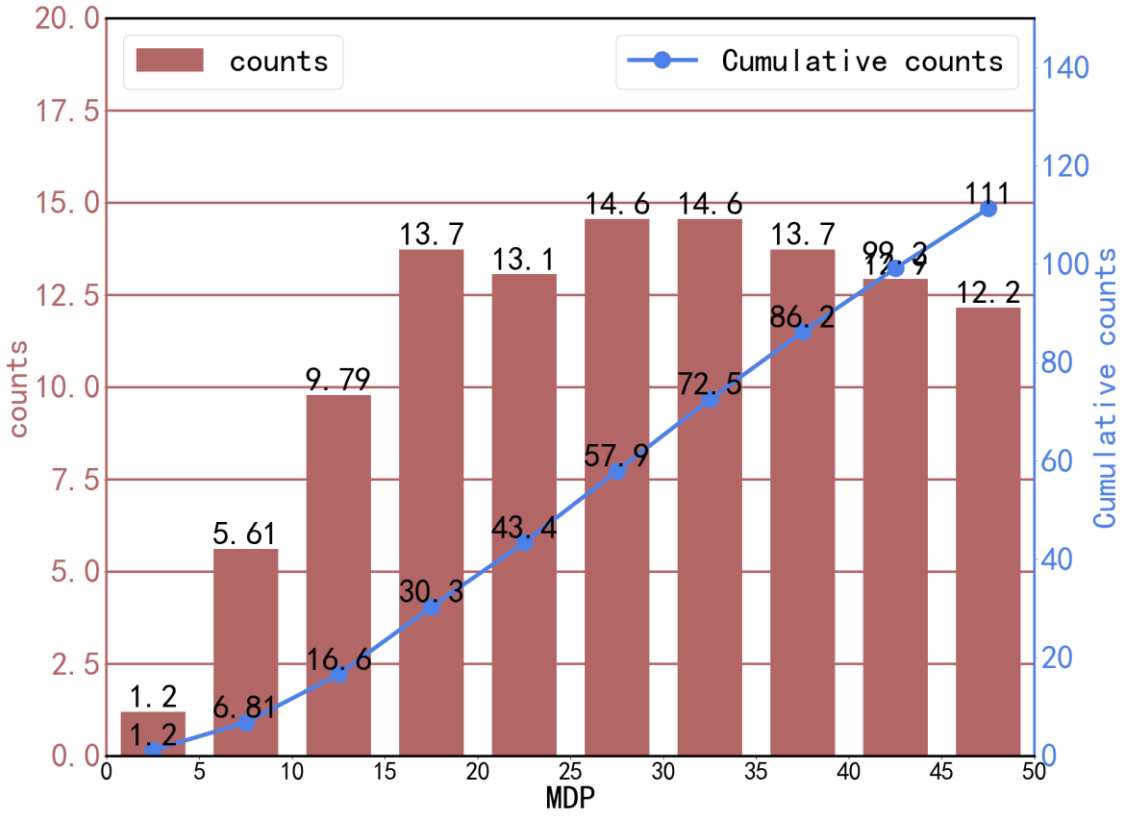

Zuke Feng et al., APJ, 2023

➢ Statistical distribution of PD
(Toma et al. 2009, Lan et al. 2021)

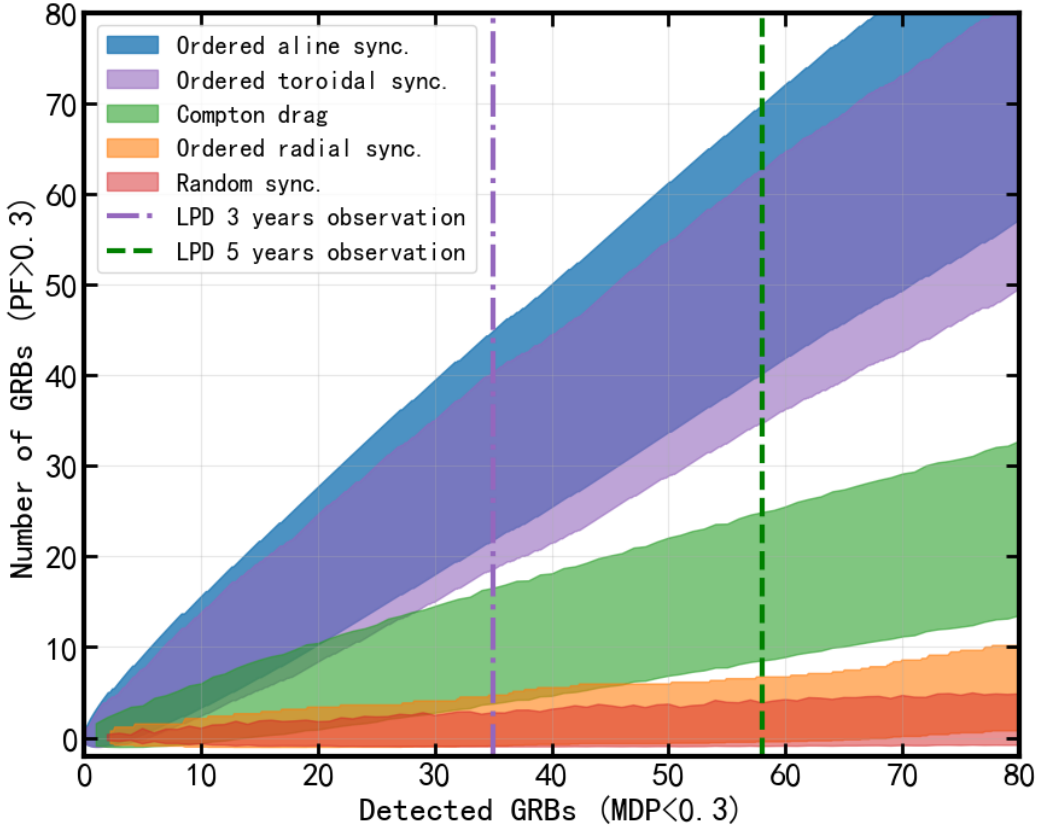

The radiation mechanism of GRBs could be determined after 5 years of observations.

X-ray polarization detector

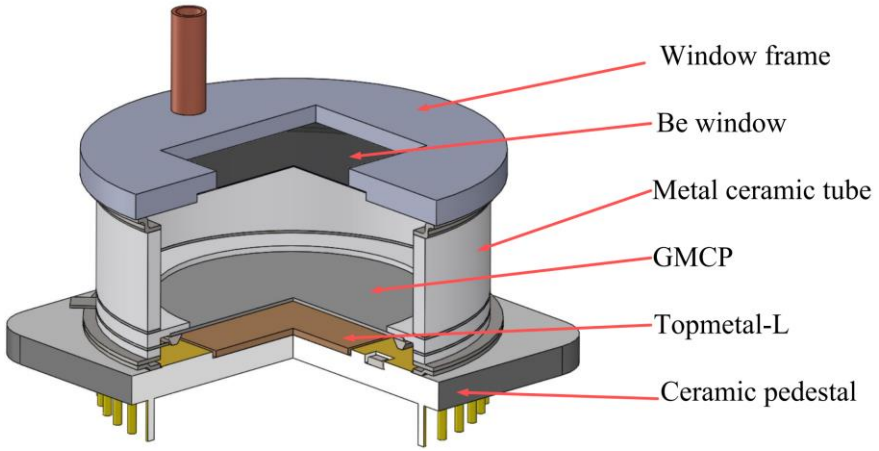

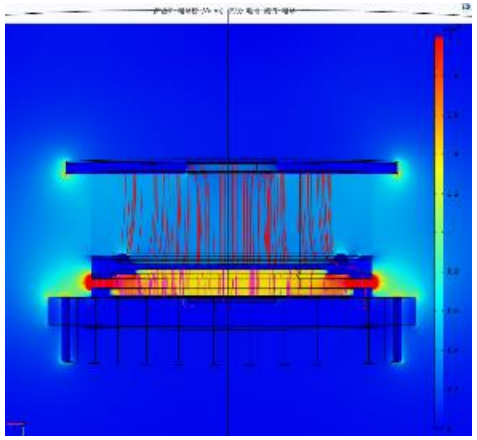

3D drawing and electric field map of the Detector.

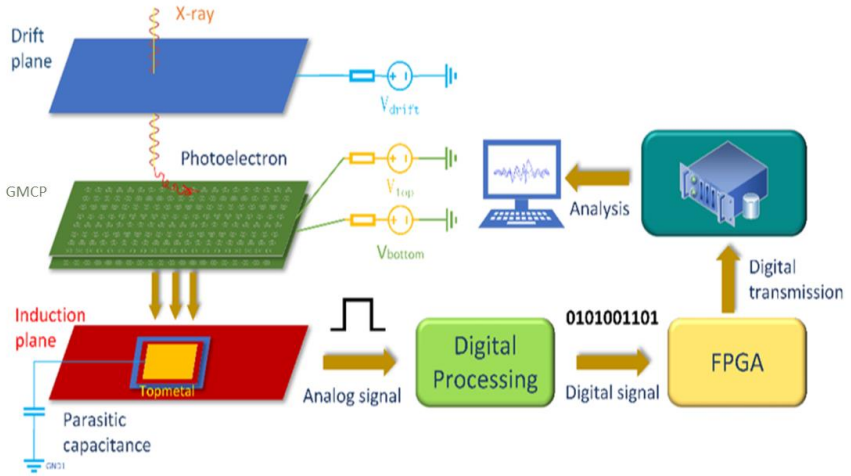

Schematic diagram of the Detector.

Performance indicators	value
Area	>3.6 cm2
Window	100 μm, beryllium
Mixture	He and DME
gas thickness	14 mm
GMCP pitch	≤60 μm
Pixels pitch	≤45 μm
Electronic noise	<40 electrons ENC
GMCP gain	>3000
Energy resolution	<20% @ 5.9 keV
Time resolution	100 μs
Modulation factor	>40% @ 4.5keV
Residual modulation factor	<1%

Huan-Bo Feng et al., Nucl. Sci. Tech, 2024
Zili Li et al., Nucl. Instrum. Meth. A , 2021
Hui Wang et al., Nucl. Sci. Tech, 2023

Gaseous Microchannel Plate (GMCP)

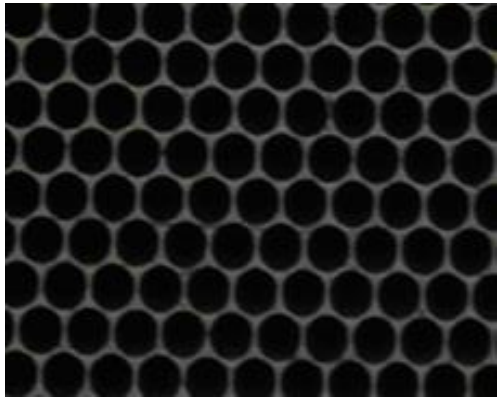

Hole diameter： 50 μm； Hole pitch： 60 μm；
Bias angle： 0°； Thickness： 400 μm；
Bulk resistance： 5 GΩ
A total of 85 units of GMCP with 15 different parameter configurations were developed.

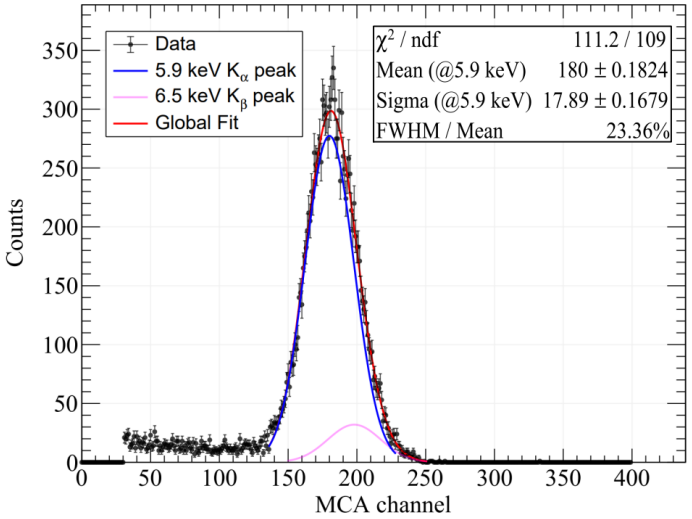

^{55}Fe X-ray spectrum

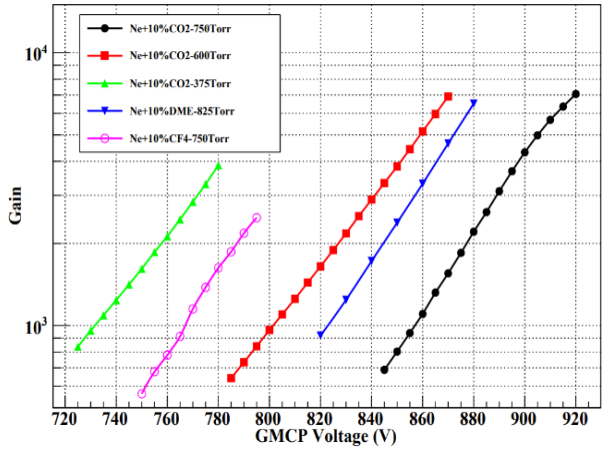

Gain curves for the GMCP under different gas conditions.

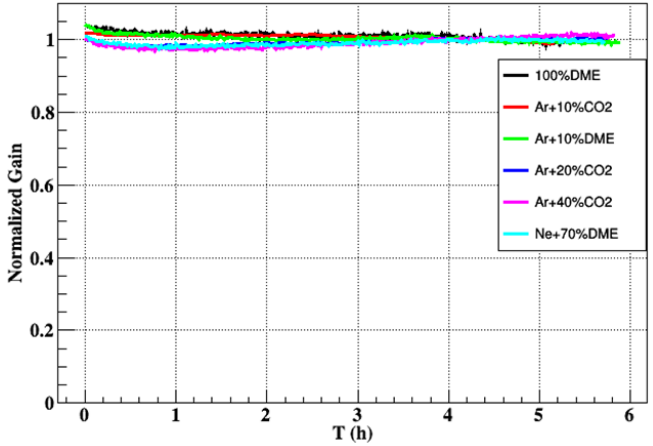

Gain stability of the GMCP in different working gases.

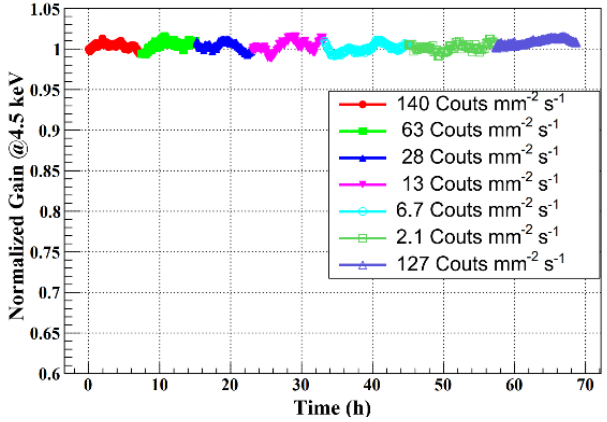

At different counting rates, the relative gain of the GMCP varies with time.

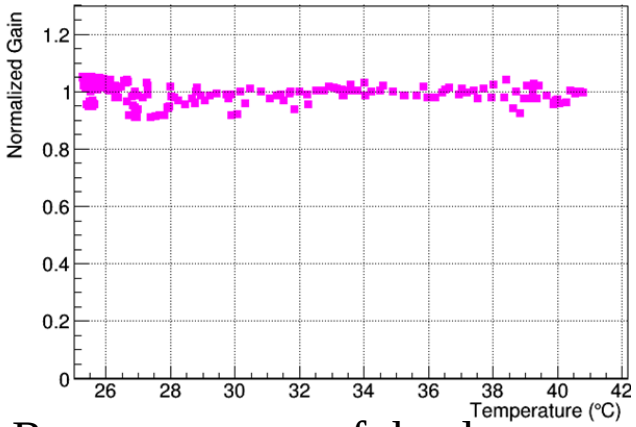

Response curve of the detector gain to temperature.

Huanbo Feng et al., Nucl. Instrum. Meth. A , 2023

Topmetal Chip

	Topmetal-II⁻	Topmetal-M1/M2	Topmetal-L
Chip Size /mm²	6 × 6	18 × 23	17 × 24
Pixel Array	72 × 72	400 × 512	356 × 512
Pixel Size /um²	83 × 83	45 × 45	45 × 45
Pixel Electrode / um²	15 × 15	10 × 20	26 × 26
ENC	~ 13.4e-	~ 15.4e-	~ 20.0e-
Power Consumption	~ 1W @3.3V	~ 4.3W @3.3V	**~ 0.8W @3.3V**
Clock	40MHz	5MHz	20MHz
Frame Rate	2.5ms	2.4ms	0.37ms @Sentinel Readout
Readout Mode	Rolling Shutter	Rolling Shutter	Rolling Shutter **/Sentinel Readout**
Readout Channel	1	16	1

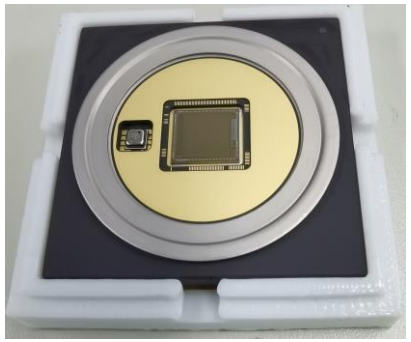

Topmetal-II⁻

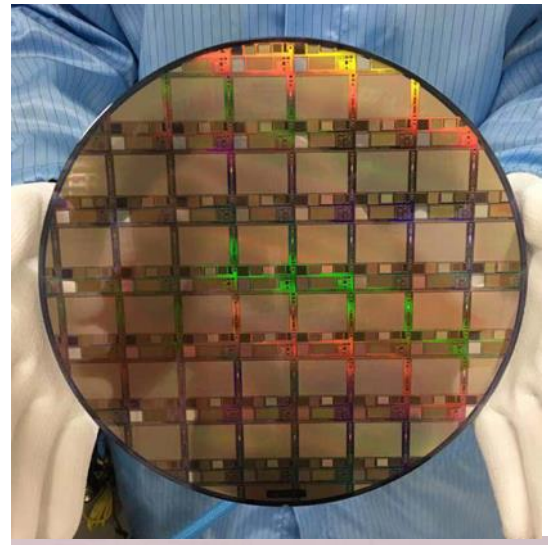

Topmetal-M1/M2

The fabrication and testing of the Topmetal-II, Topmetal-M1, Topmetal-M2 and Topmetal-L chips have been completed.

Topmetal-L and Readout

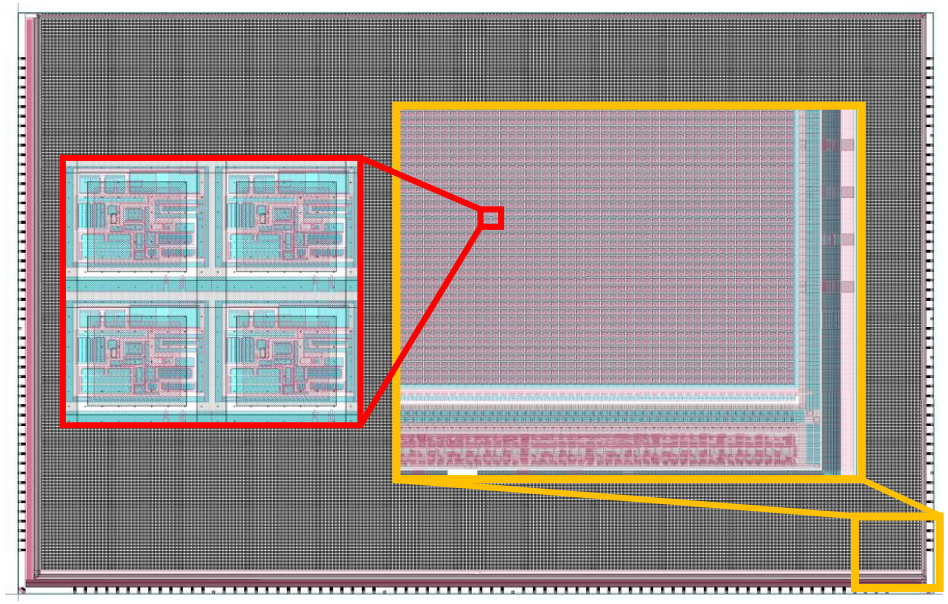

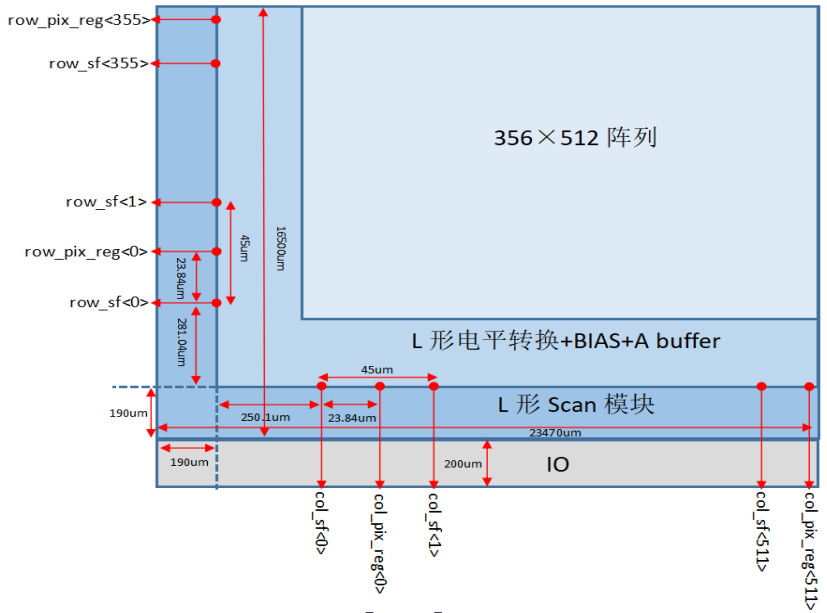

Topmetal-L layout structure.

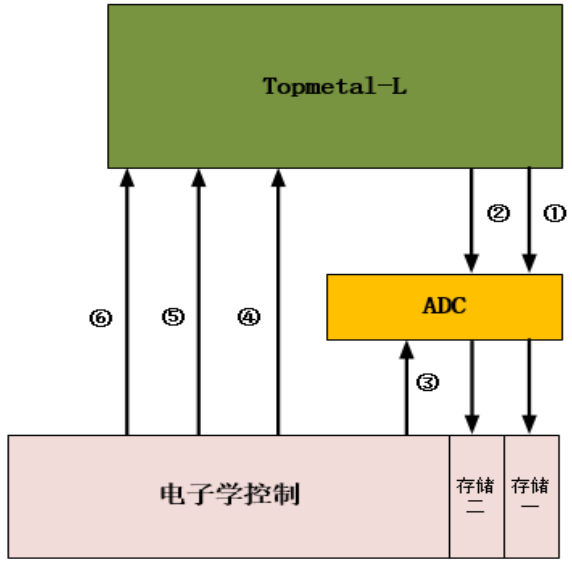

Data communication instructions.

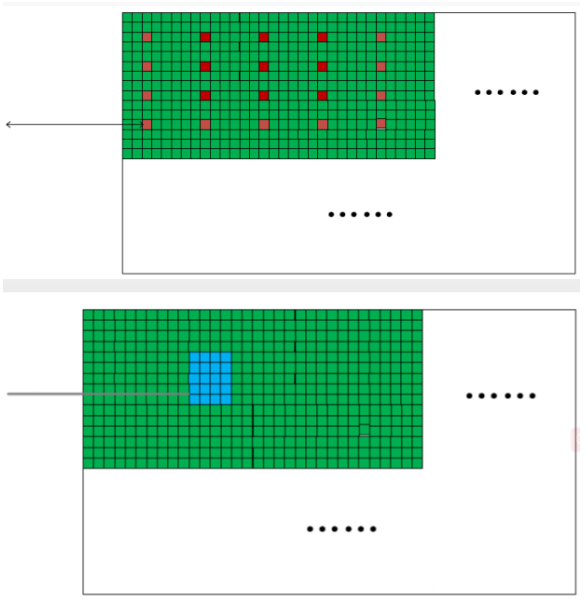

Sentry scanning and area scanning.

In the readout section of the Topmetal-L chip, a novel readout scheme called the **Sentinel readout scheme** is adopted.

GMCP & Topmetal-L Commissioning

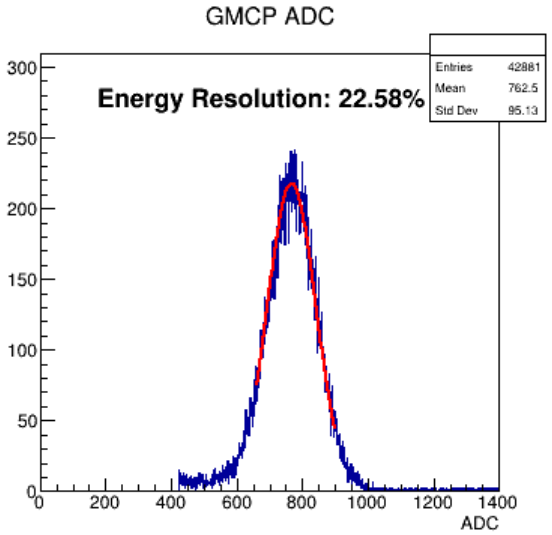

4.5 keV X-ray spectrum

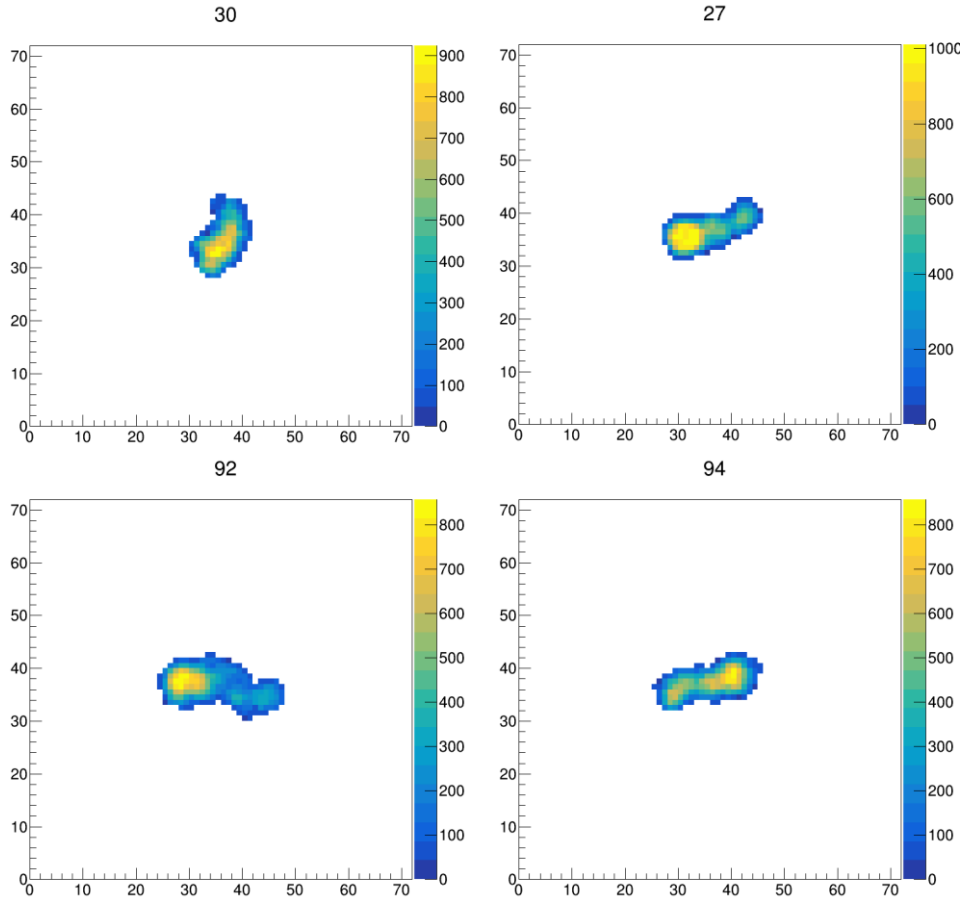

Example electron tracks produced by 5.9 keV X-rays.

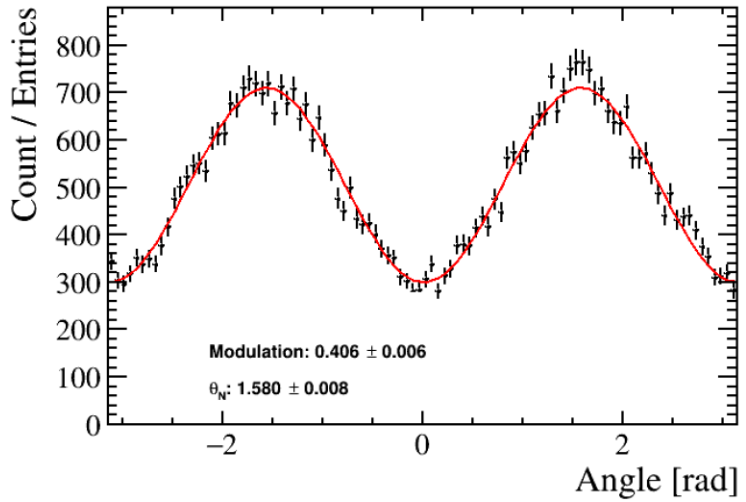

Modulation curve obtained from a 4.5 keV polarized X-ray measurements.

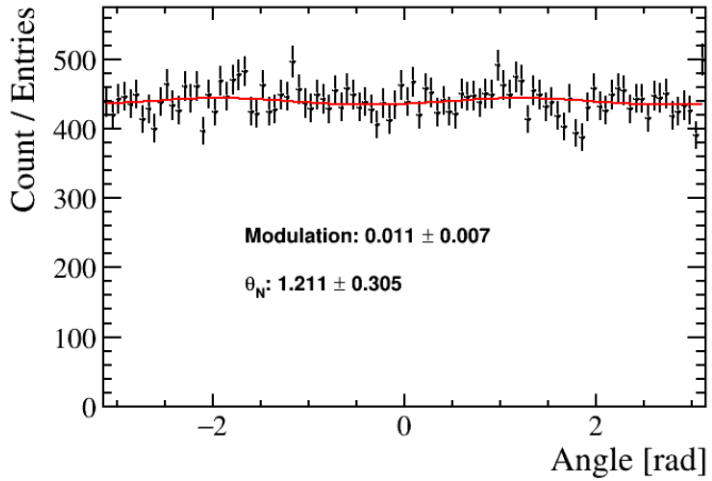

Modulation curve obtained from a 5.9 keV unpolarized X-ray measurements.

LPD Detector Unit & Electronics

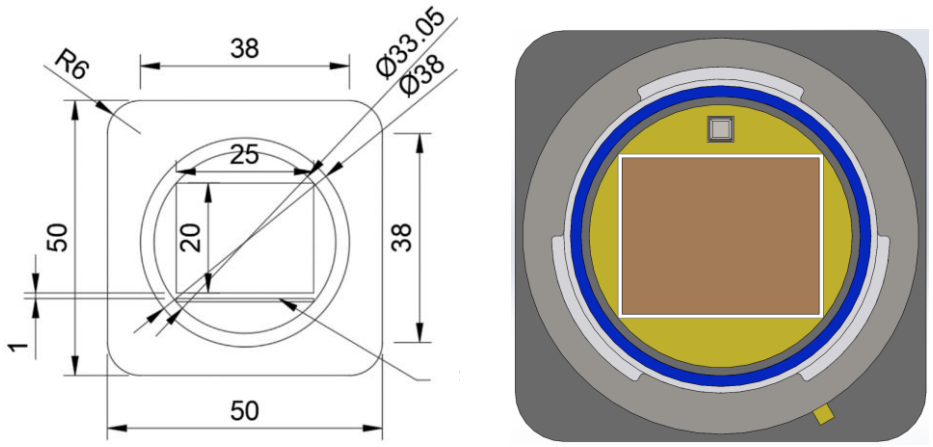

Schematic diagram of the Topmetal-L chip bonding design.

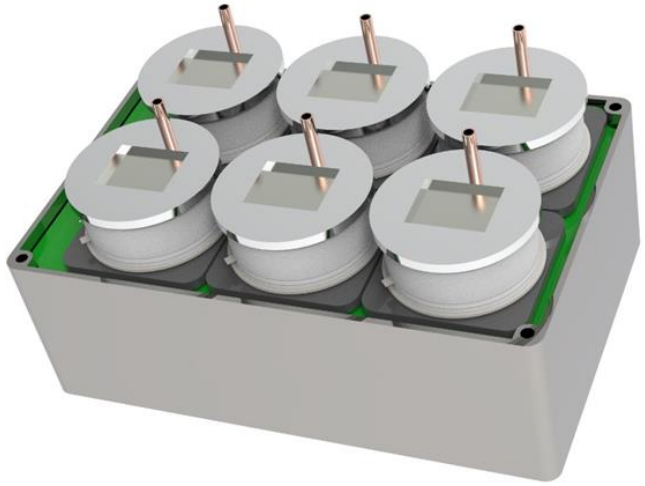

Overall diagram of the detection unit (Includes 6 Topmetal-L chips).

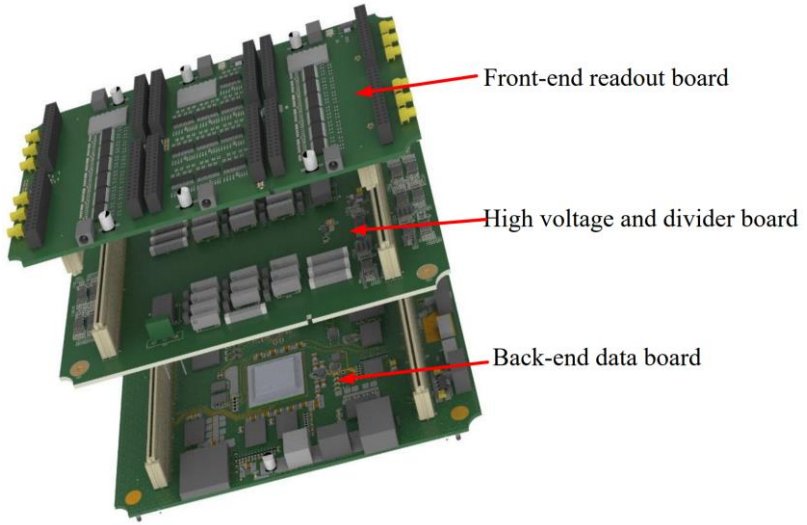

Schematic diagram of the electronics. The three boards are connected board-to-board and have the same planar structure.

	Data volume（Day）
Particle background	1GB
Diffuse photon background	65.29 GB
Normal GRB	0.80 GB
Ultra-intense GRB	39.83 GB
Total data volume	81.81GB

The estimation of data volume for the LPD detector.

Flight validation of LPD prototype

Cosmic X-ray Polarimeter Detection (CXPD) CubeSat

* Validation of soft X-ray polarization detection technology
* Spatial background measurement
* Standard X-ray source polarization measurement

Size： $96 * 96 * 108\ mm^3$
Mass： ~900 g
Power consumption： <5 W

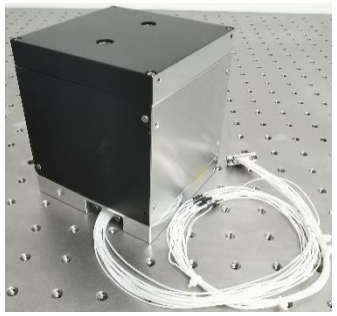

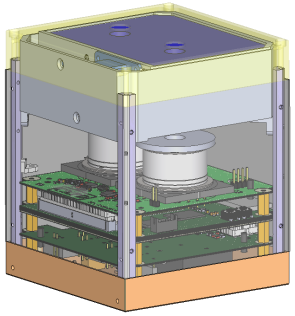

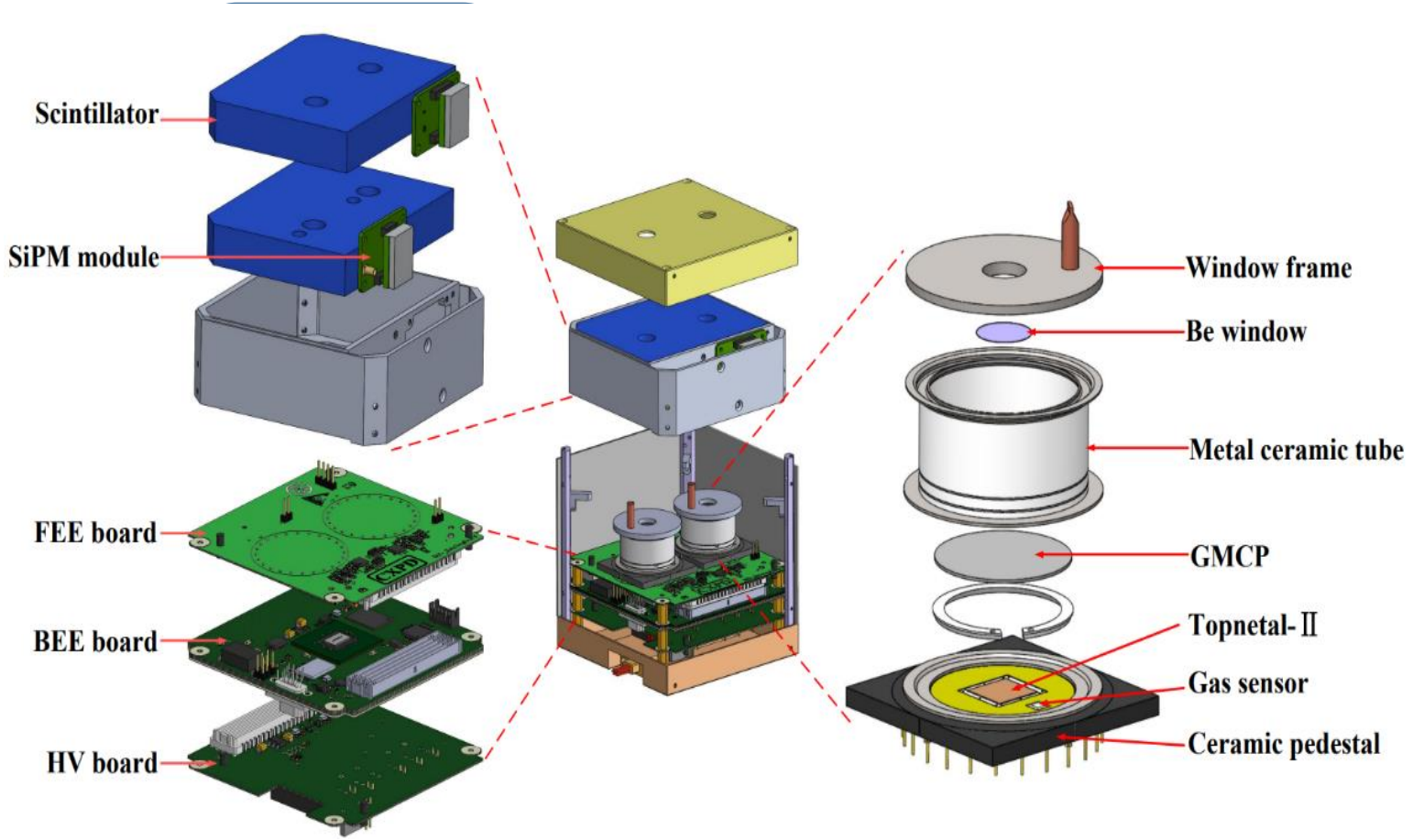

LPD prototype

照

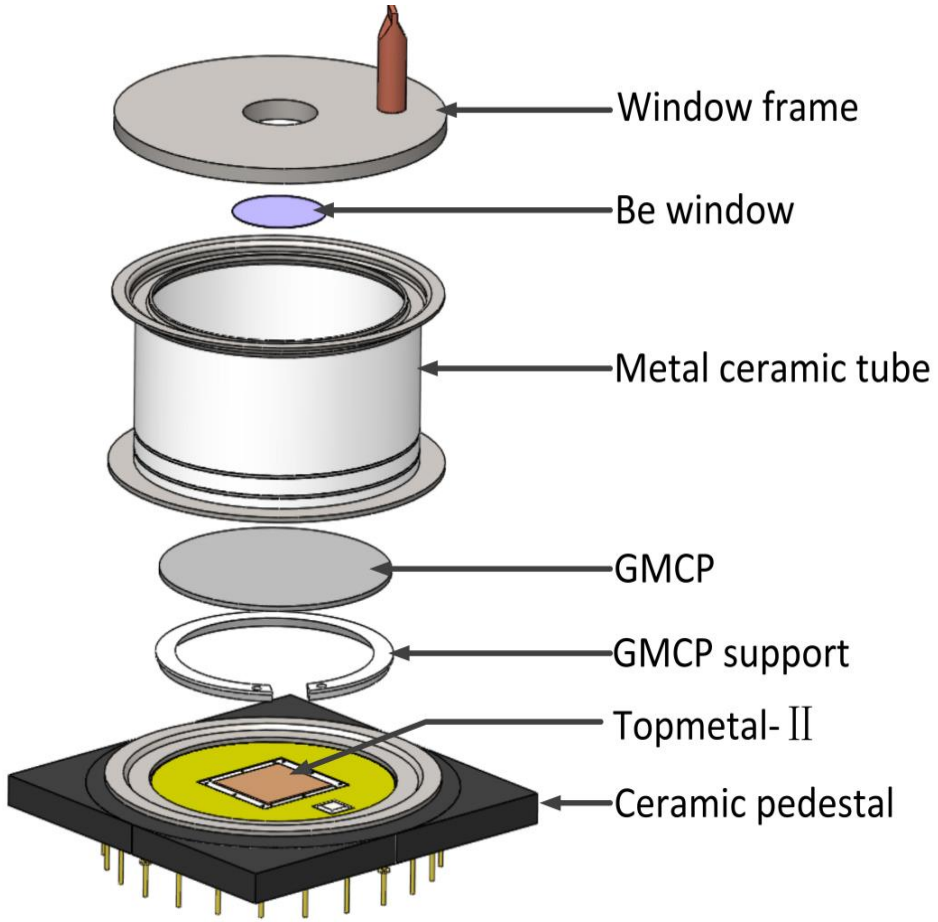

A schematic drawing of the GMPD

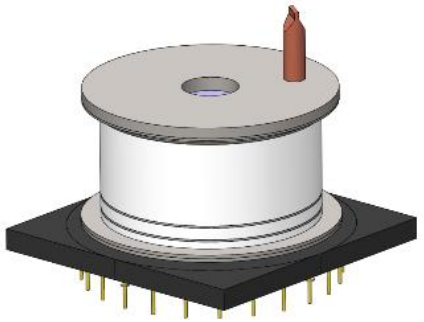

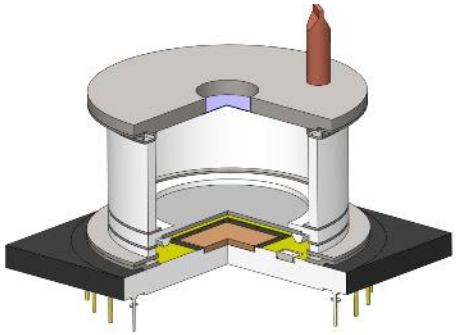

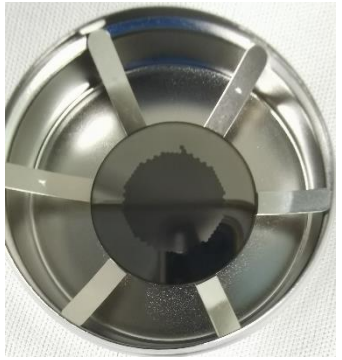

Gas Microchannel Plate (GMCP):
Hole pitch : 60 μm
Hole diameter : 50 μm
Effective diameter： 12 mm

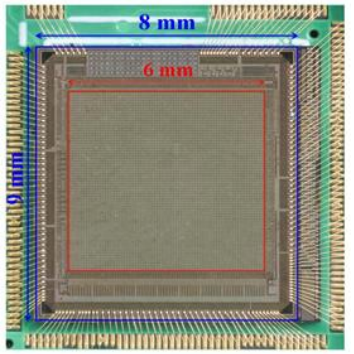

Topmetal-II：
Pixel pitch :83 μm
Pixel arrays :72×72
Effective area： 6×6 mm2

Assembling of gas detectors

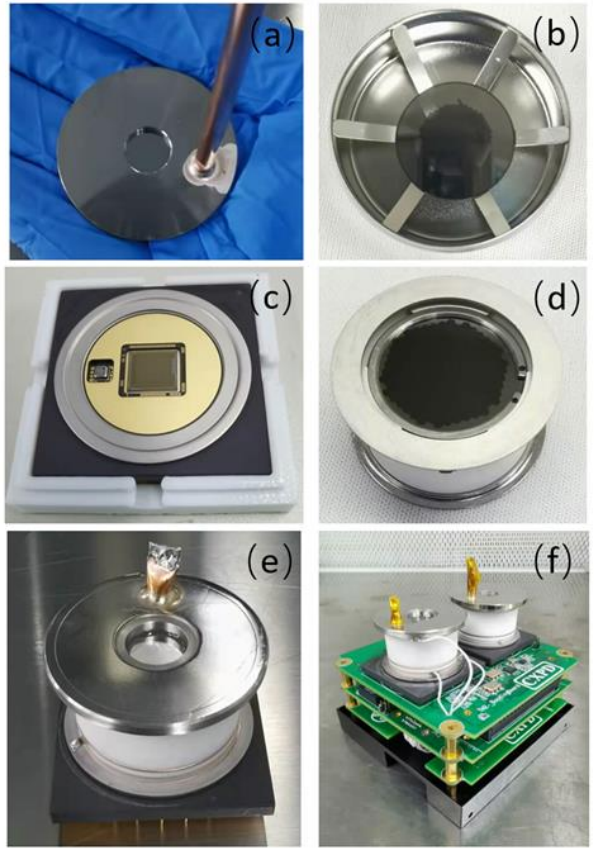

Materials with low outgassing rates: ceramics, alloys, beryllium, glass, etc.
Welding technology: brazing, laser welding, ultrasonic welding.

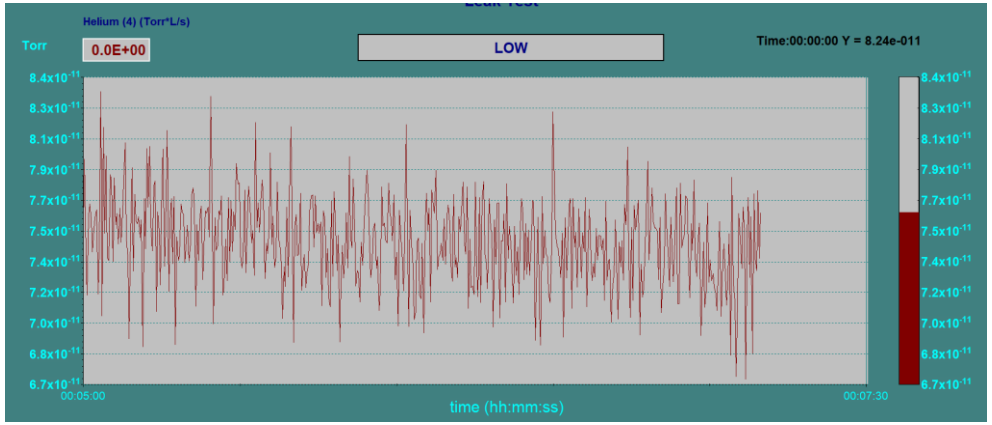

Leakage rate： 7.6^{-11} Torr*L/s

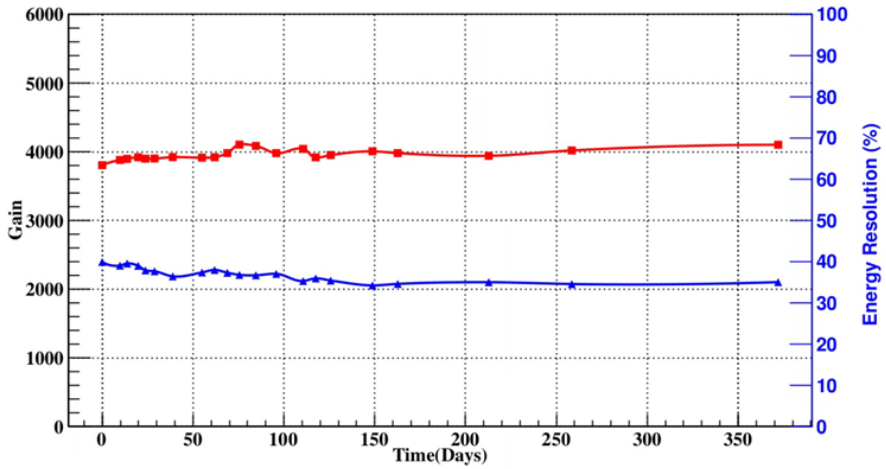

Long-term monitoring of the detector’s normalized gain (Red) and energy resolution (Blue).

GMCP bottom amplifier circuit

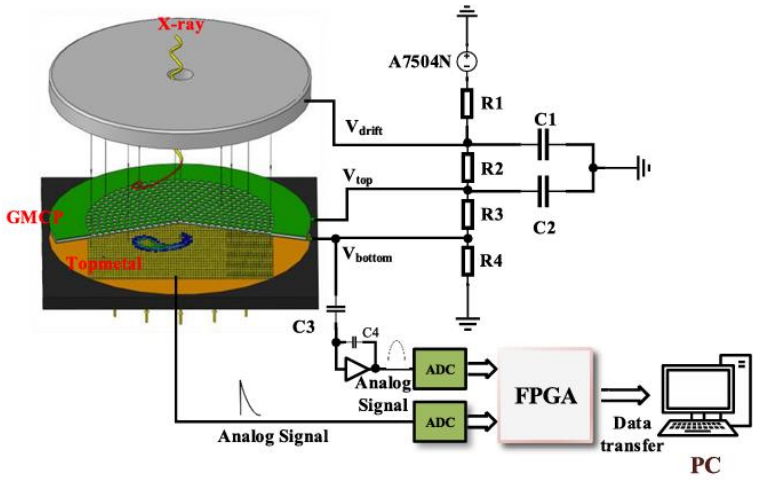

Schematic of the GMPD experimental system.

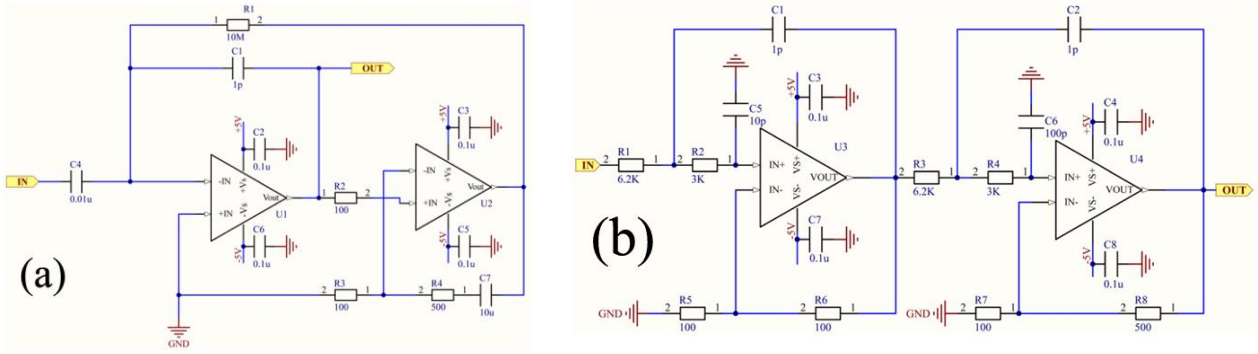

GMCP's bottom amplifier circuit. (a) CSA. (b) Filter shaper.

- Improve the time resolution and energy resolution.

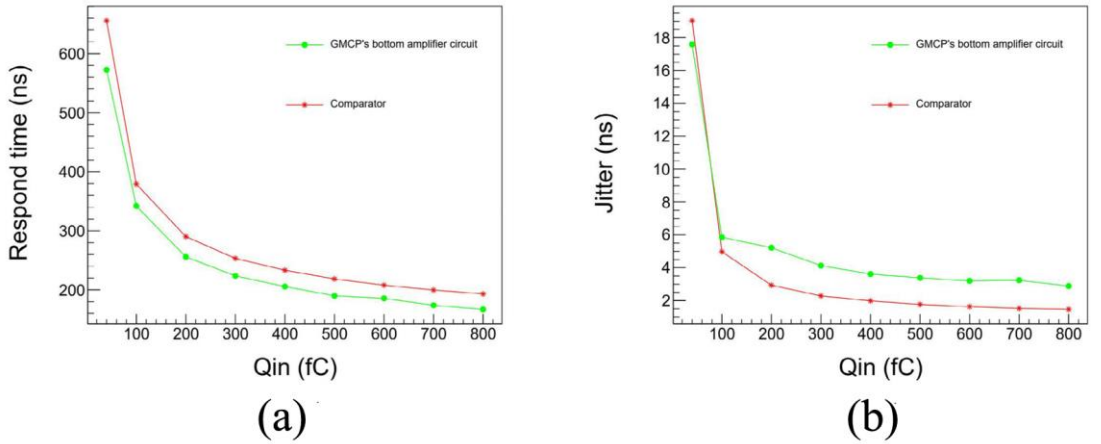

Time performance of the GMCP's bottom amplifier circuit. (a) Time walk. (b) Time accuracy.

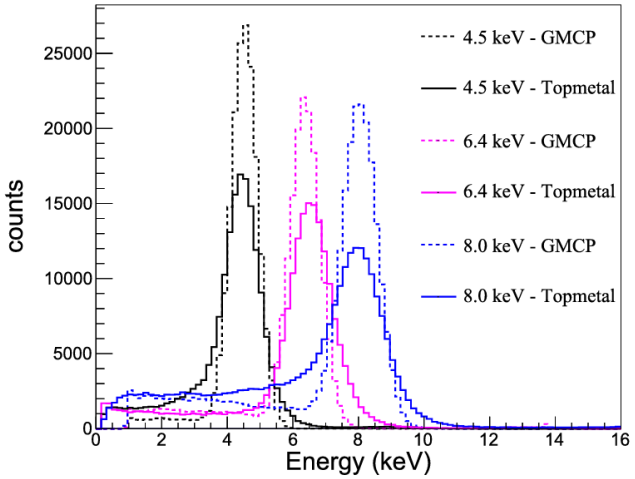

Energy spectrum of GMCP and Topmetal-II after events matching.

Zongwang Fan et al., IEEE Trans, 2023

Polarized X-ray measurements

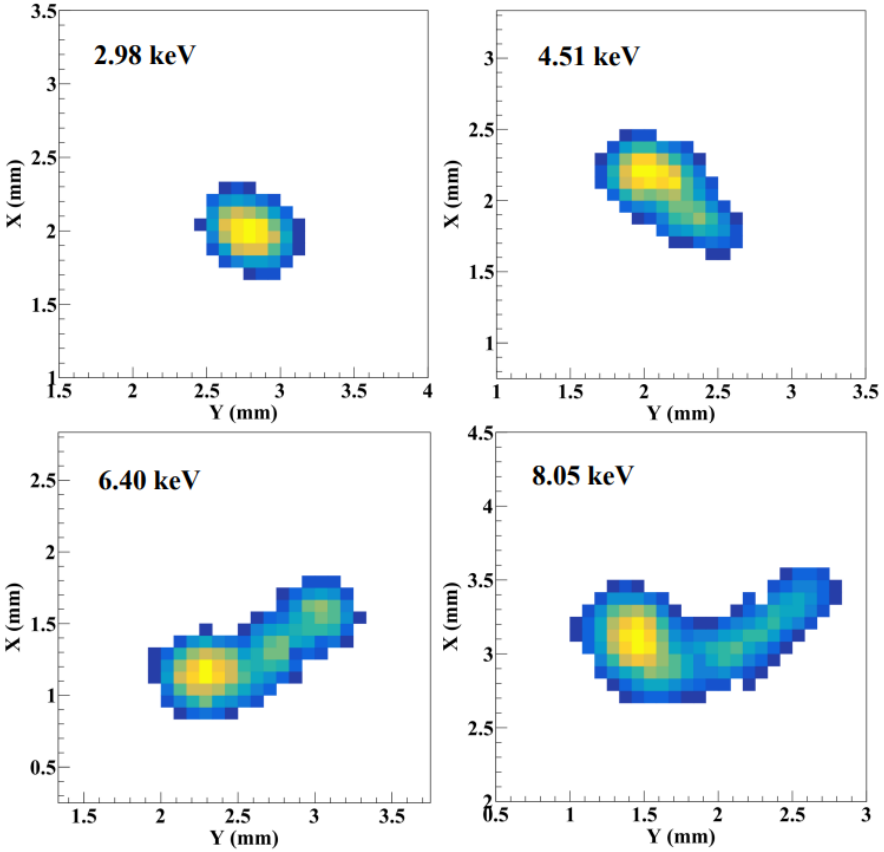

Example electron tracks produced by X-rays of different energies.

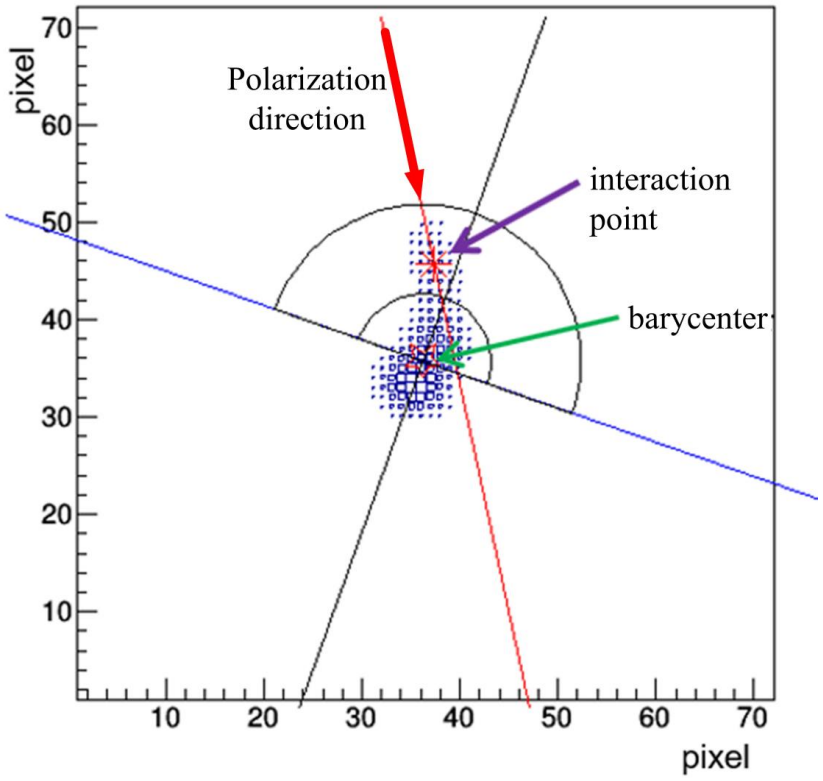

Schematic diagram of photoelectron track reconstruction.

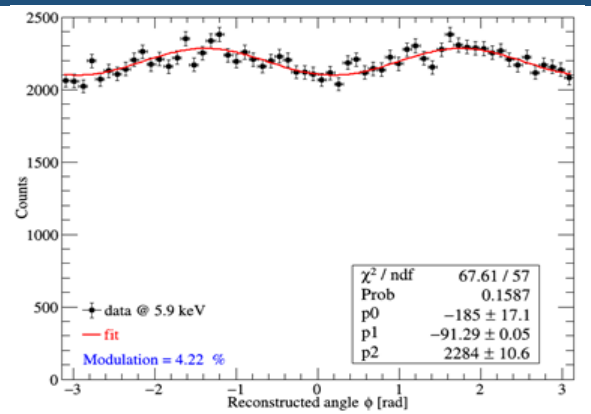

Modulation curve obtained from a 5.9 keV unpolarized X-ray measurements.

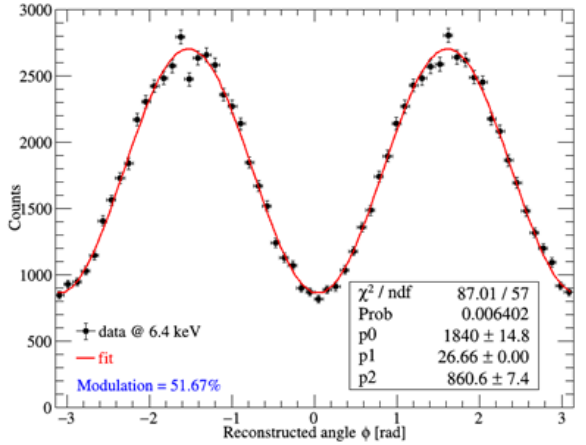

Modulation curve obtained from a 6.4 keV polarized X-ray measurements.

Xuefeng Huang et al., Nucl. Sci. Tech, 2021

X-ray polarized calibration platform

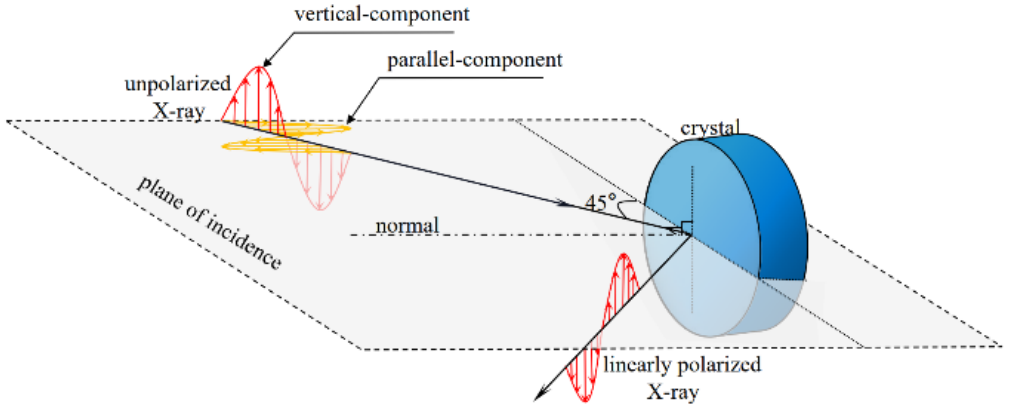

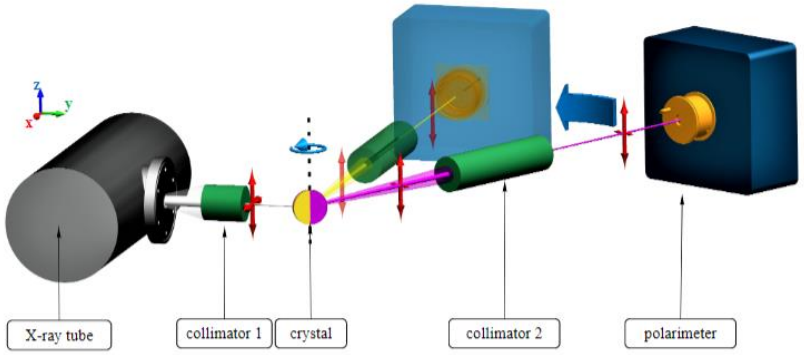

Schematic diagram of the principle of polarized X-ray source based on Bragg diffraction.

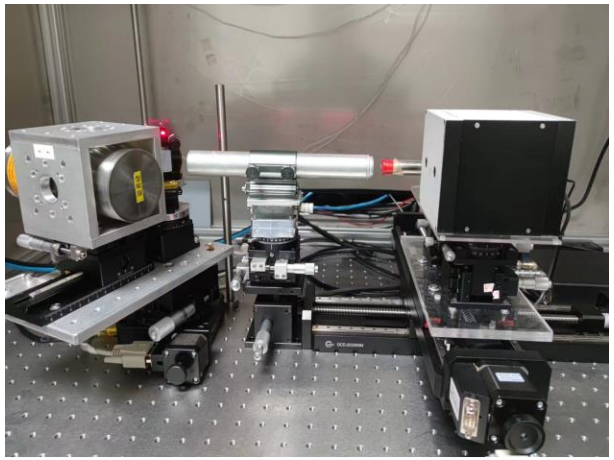

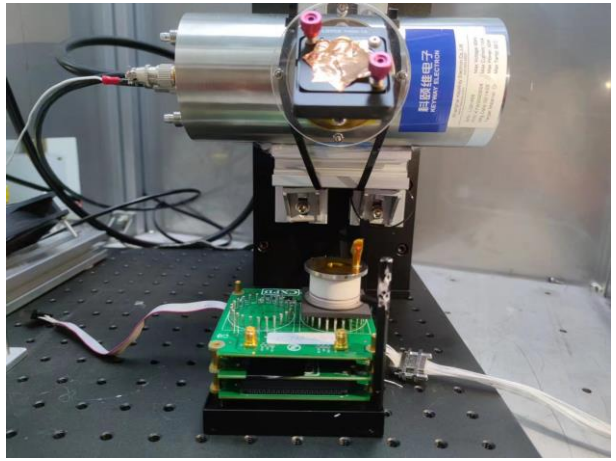

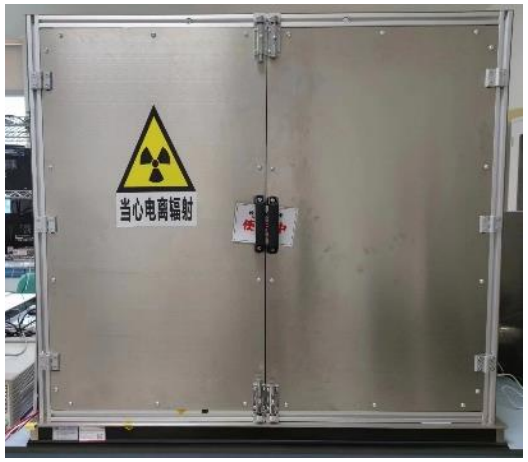

X-ray polarization calibration platform set up in the laboratory.

X-ray polarized calibration platform

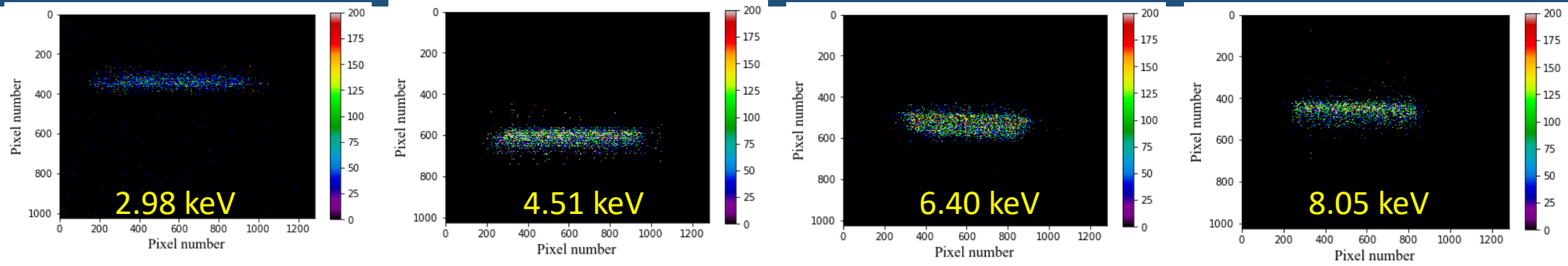

Image with the CCD imager of the photons generated with the polarized source.

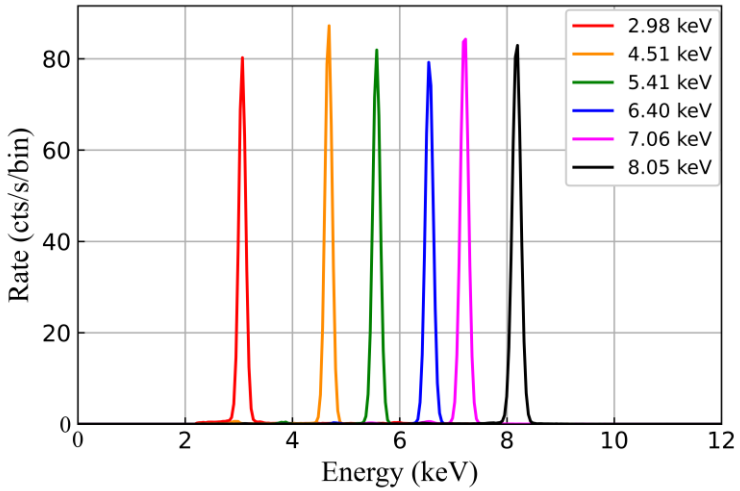

Spectrum of the polarized source.

TABLE II. Configurations and performance list of 8.05 keV linear polarized sources. The polarization degree is calculated using Eq. (3).

Energy(keV)	2.98	4.51	5.40	6.40	7.06	8.05
Crystal	Si(111)	Si(220)	Si(311)	Si(400)	Si(331)	Si(224)
Incident radiation	Ag L_α	Ti K_α	Cr K_α	Fe K_α	Fe K_β	Cu K_α
Diffraction angle(deg)	41.6	45.8	44.5	45.5	44.9	44.1
Rate(cts/s)	207.52	375.49	370.49	375.8	426.77	439.25
Proportion of monochromatic light[a](%)	93.04	97.91	98.31	98.64	97.40	97.32
FWHM(eV)	139.38	146.69	149.39	142.42	158.62	159.73
X-ray tube settings	8.0 kV, 0.49 mA	6.5 kV, 0.19 mA	7.0 kV, 0.19 mA	8.0 kV, 0.31 mA	9.8 kV, 0.44 mA	9.5 kV, 0.58 mA
Polarization(%)	97.4	99.8	99.9	99.8	99.9	99.8

[a] The proportion of monochromatic light is defined as the ratio of the number of photons falling within three times the sigma of the target peak centre value to the total photons.

TABLE III. Configurations and performance list of 8.05 keV partially polarized sources. The copper Kα characteristic line diffracted by silicon crystal to generate beams with different degrees of polarization. The polarization degree is calculated using Eq. (3).

Energy(keV)	8.05	8.05	8.05	8.05	8.05	8.05
Crystal	Si(111)	Si(220)	Si(311)	Si(400)	Si(331)	Si(224)
Incident radiation	Cu K_α	Cu K_α	Cu K_α	Cu K_α	Cu K_α	Cu K_α
Diffraction angle(deg)	14.2	23.7	28.1	34.6	38.2	44.1
Rate(cts/s)	277.75	166.66	224.14	657.92	146.97	555.92
Proportion of monochromatic light[a](%)	92.82	96.84	98.32	98.40	98.36	98.37
FWHM(eV)	193.05	162.63	159.61	159.24	159.11	159.73
X-ray tube settings	9.3 kV, 0.19 mA	9.4 kV, 0.39 mA	10.3 kV, 0.19 mA	11.5 kV, 0.29 mA	10.0 kV, 0.19 mA	10.5 kV, 0.29 mA
Polarization(%)	12.8	37.0	52.6	77.5	89.5	99.8

[a] The proportion of monochromatic light is defined as the ratio of the number of photons falling within three times the sigma of the target peak centre value to the total photons.

Yanjun Xie et al., EXP ASTRON, 2023

Spectral and polarimetric characterization

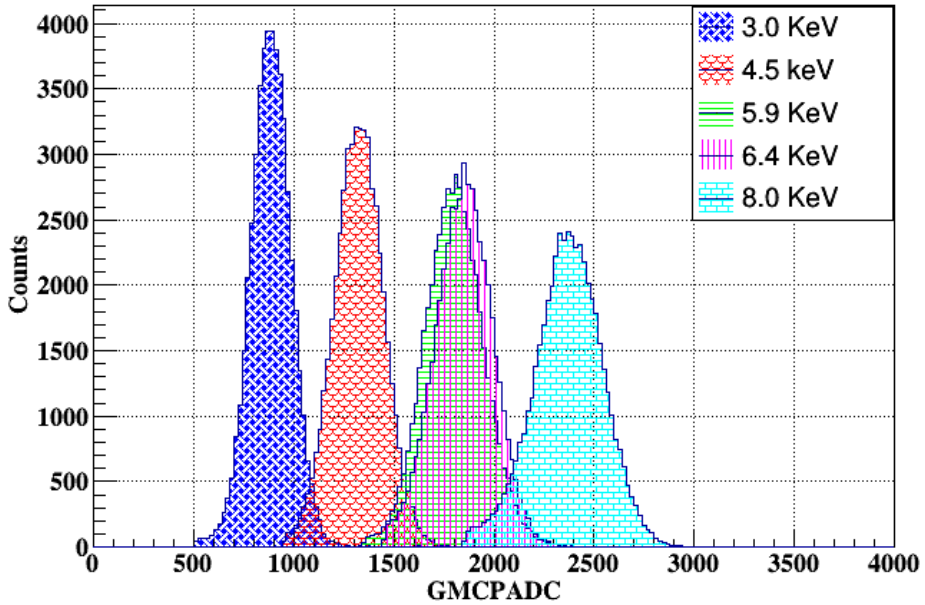

Energy spectra measured with Bragg diffractions.

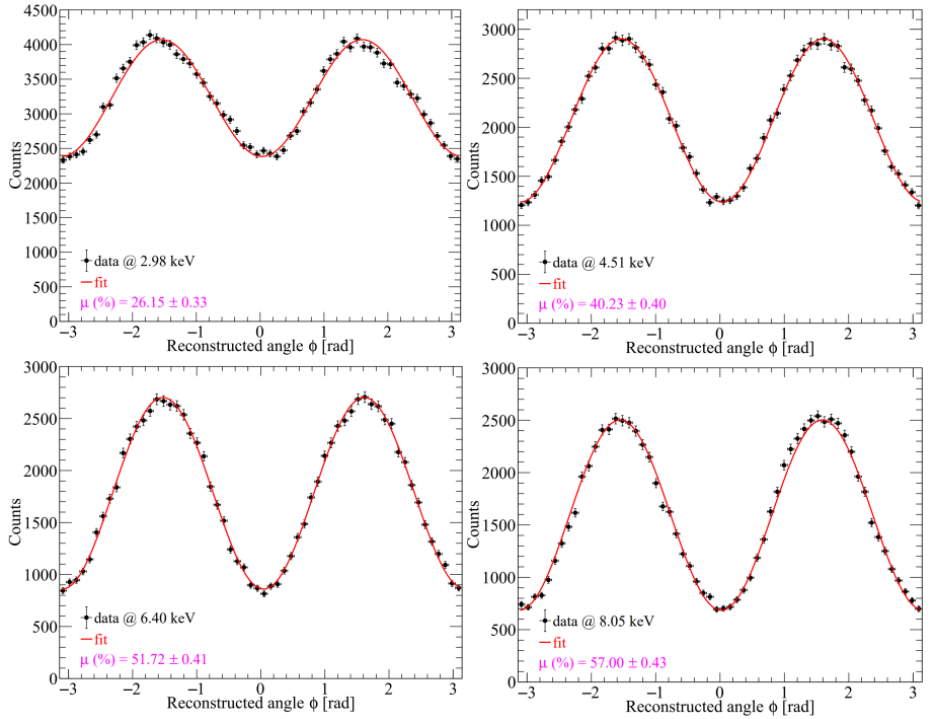

Modulation curves measured with Bragg diffraction.

Energy (keV)	E_{peak} (ADC)	FWHM (ADC)	FWHM/E_{peak}
2.98	885.5 ± 0.5	230.3 ± 0.9	0.260 ± 0.002
4.51	1323.1 ± 0.6	285.0 ± 1.1	0.215 ± 0.001
6.40	1880.1 ± 0.7	338.9 ± 1.4	0.180 ± 0.001
8.05	2369.6 ± 0.9	190.1 ± 1.7	0.165 ± 0.001

GMPD, 40%He+60%DME, 0.8 atm		
Energy (keV)	μ	$\mu\sqrt{\varepsilon}$
2.98	0.2615 ± 0.0033	0.0753
4.51	0.4023 ± 0.0040	0.0749
6.40	0.5172 ± 0.0041	0.0608
8.05	0.5700 ± 0.0043	0.0486

Huanbo Feng et al., JINST, 2023

Calibration for different Polarimetry directions

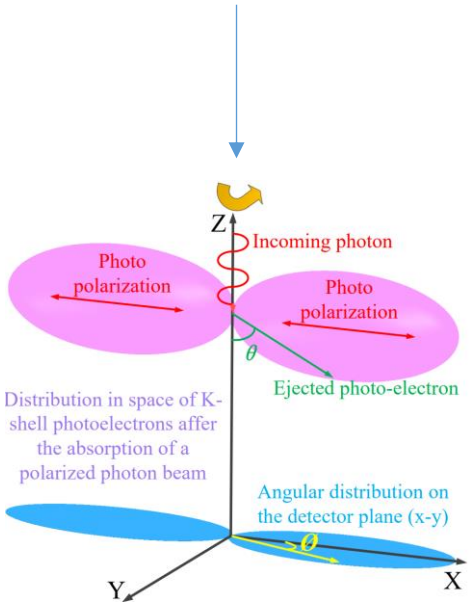

Rotation of the detector along the incident beam.

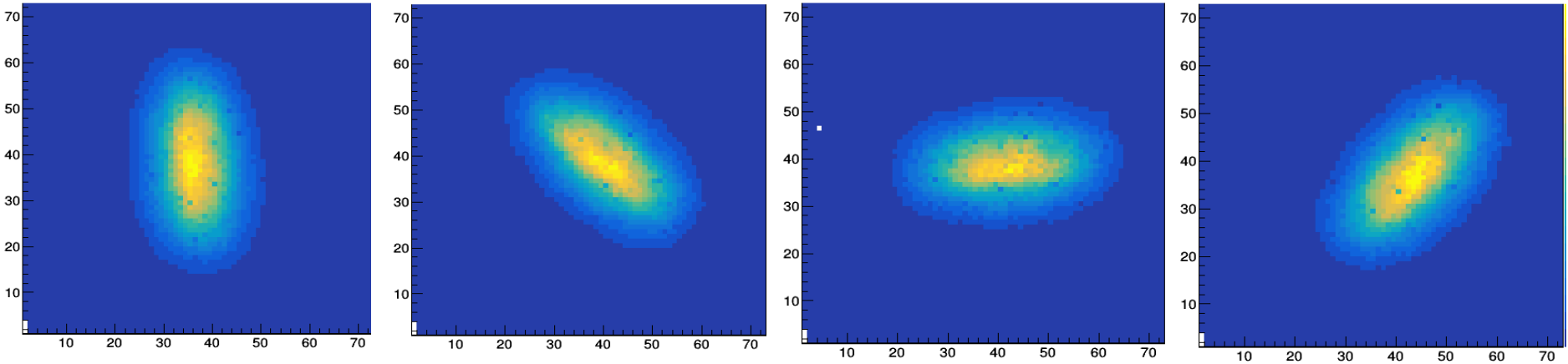

Rotation angle: 0°

Rotation angle: 45°

Rotation angle: 90°

Rotation angle: 135°

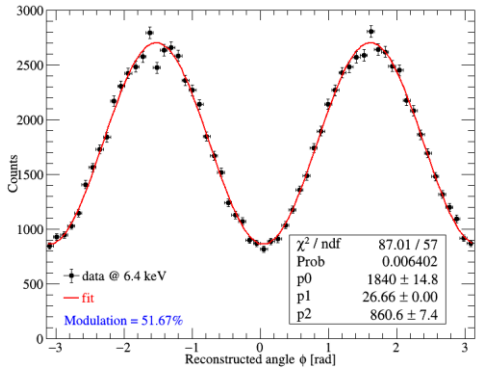

modulation factor: 51.67%

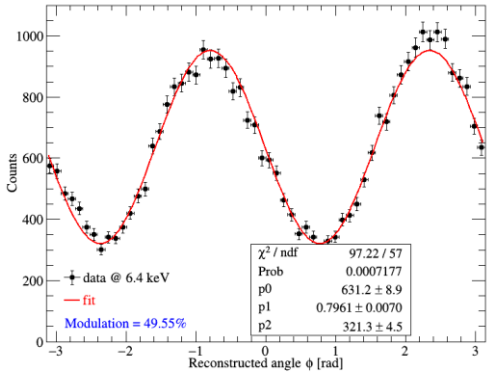

modulation factor: 49.55%

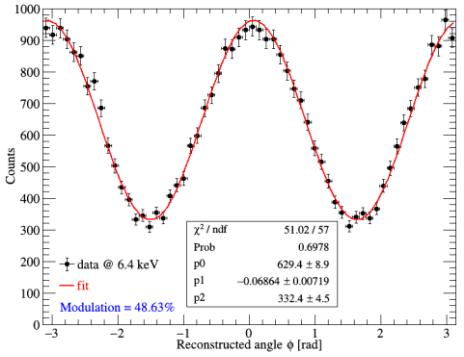

modulation factor: 48.63%

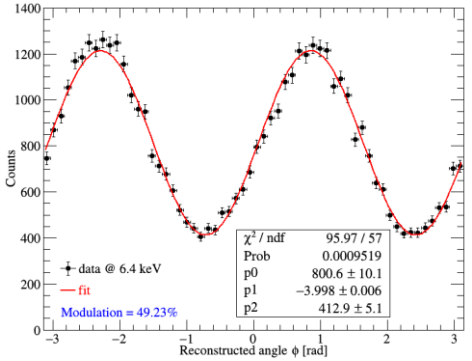

modulation factor: 49.23%

Calibration of the oblique incidence

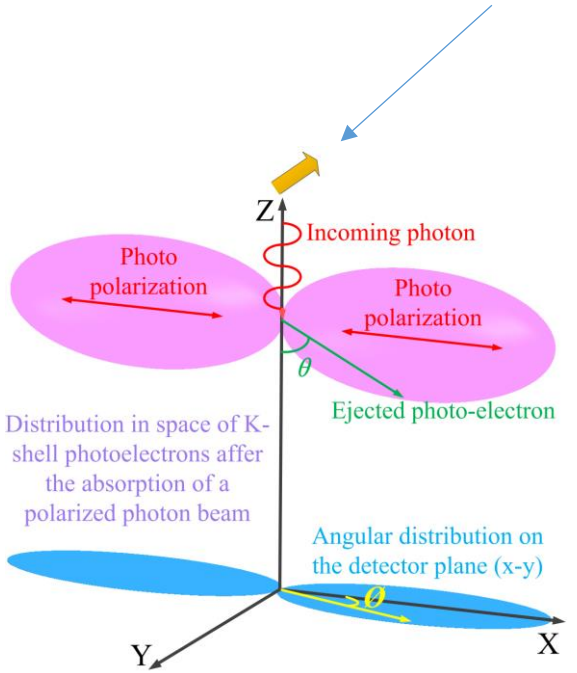

Inclined direction perpendicular to the direction of polarization.

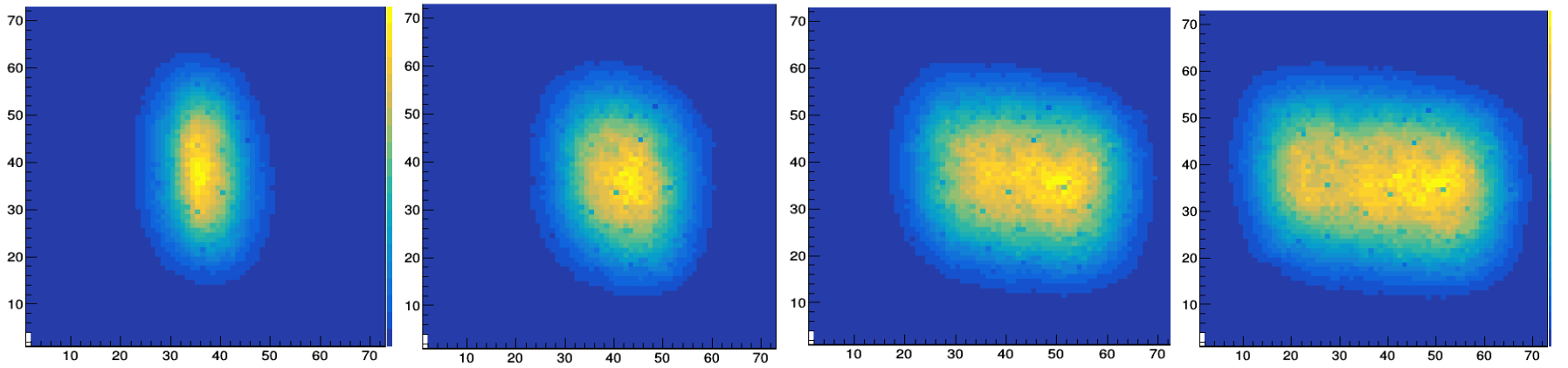

Inclined angle： 0° Inclined angle： 5° Inclined angle： 10° Inclined angle： 13°

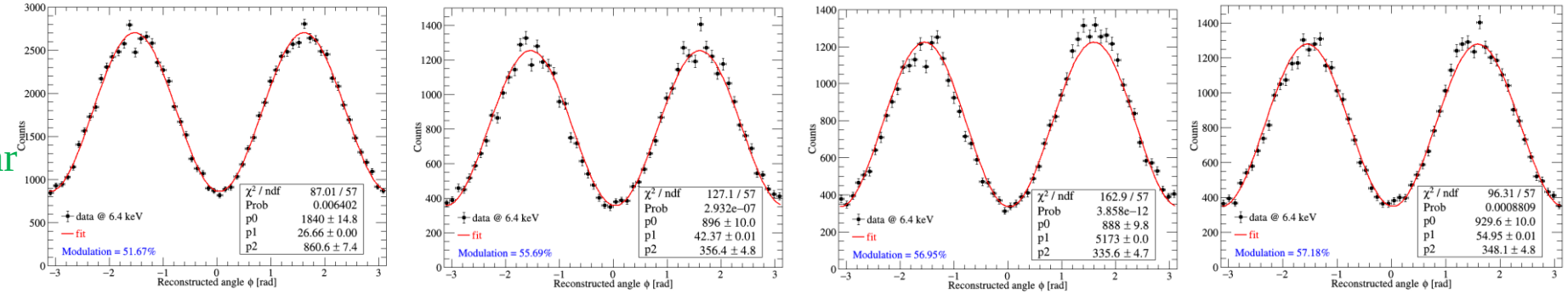

modulation factor : 51.67%

modulation factor : 55.69%

modulation factor : 56.95%

modulation factor : 57.18%

Calibration of the oblique incidence

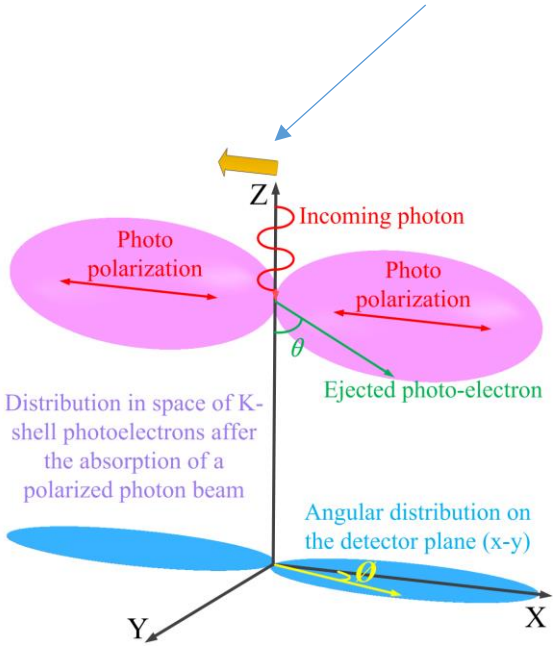

Inclined direction parallel to the direction of polarization.

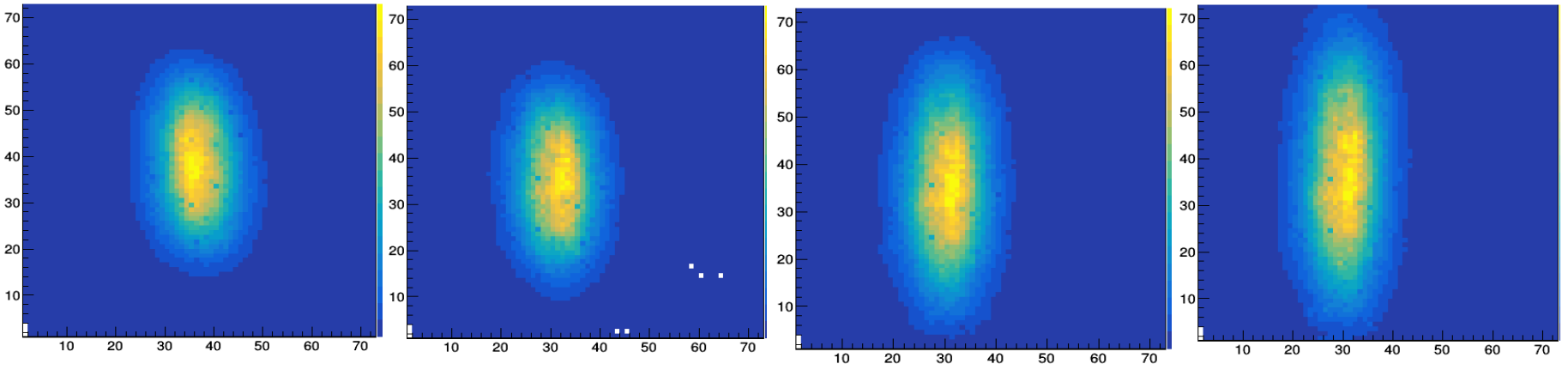

Inclined angle： 0° Inclined angle： 5° Inclined angle： 10° Inclined angle： 13°

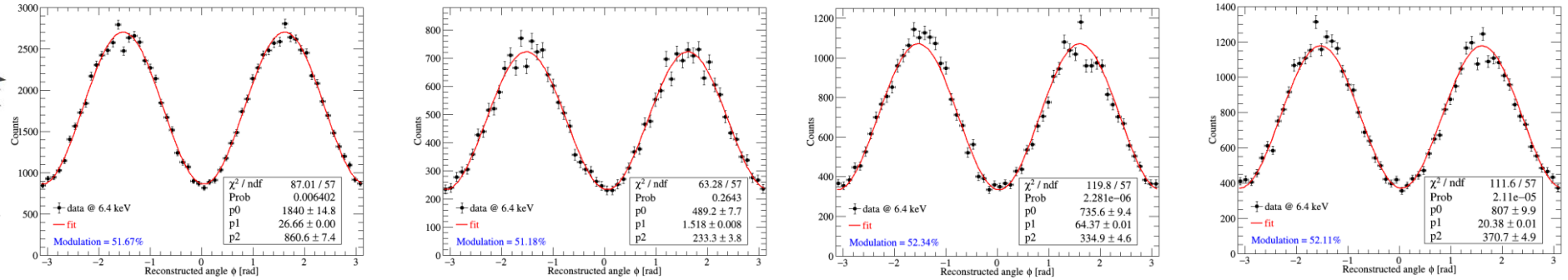

modulation factor : 51.67%

modulation factor : 51.18%

modulation factor : 52.34%

modulation factor : 52.11%

Assembly and testing of CXPD payload

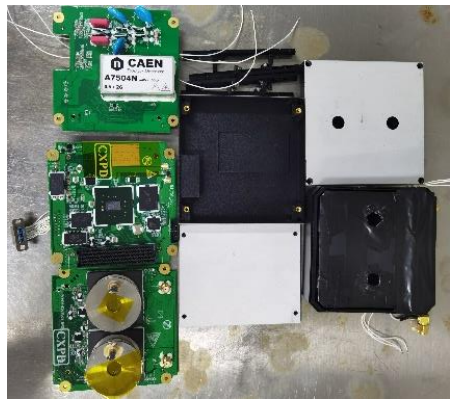

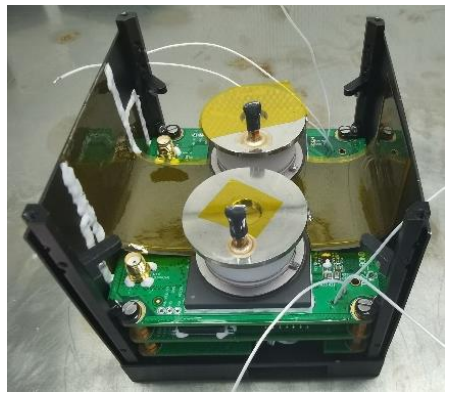

Assembly process of the CubeStar payload

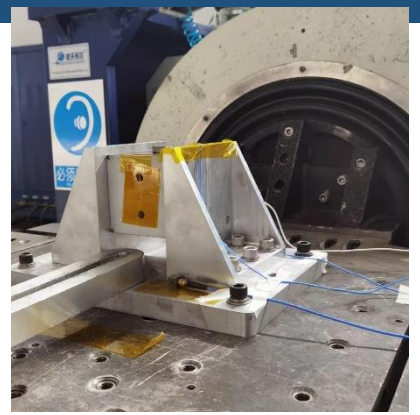

Vibration test

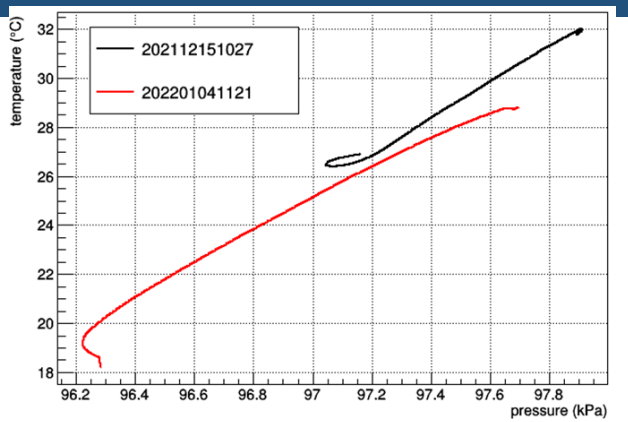

照

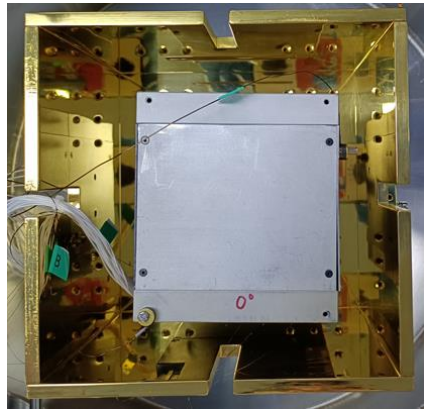

Thermal vacuum test

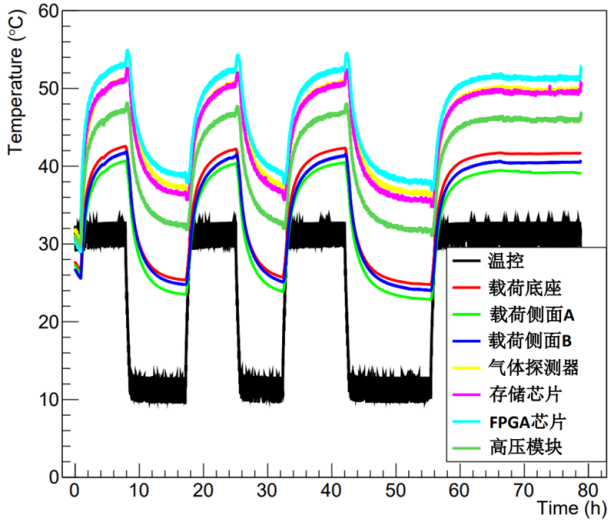

Status of CXPD payload

The CXPD payload was delivered in February 2023.

On May 10th, the installation and testing of the CXPD payload with the CubeSat were completed.

On June 7th, the CXPD payload was successfully launched along with the CubeSat.

Status of CXPD payload

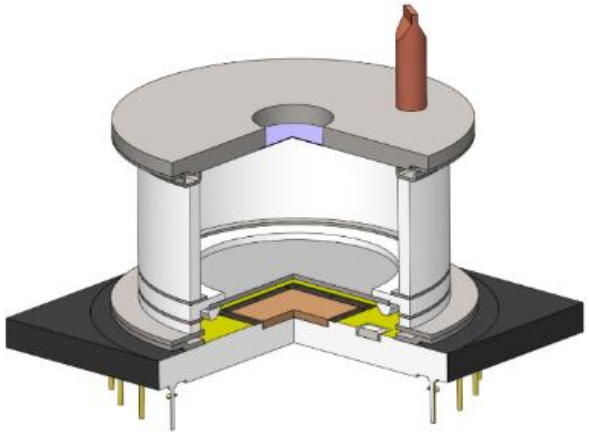

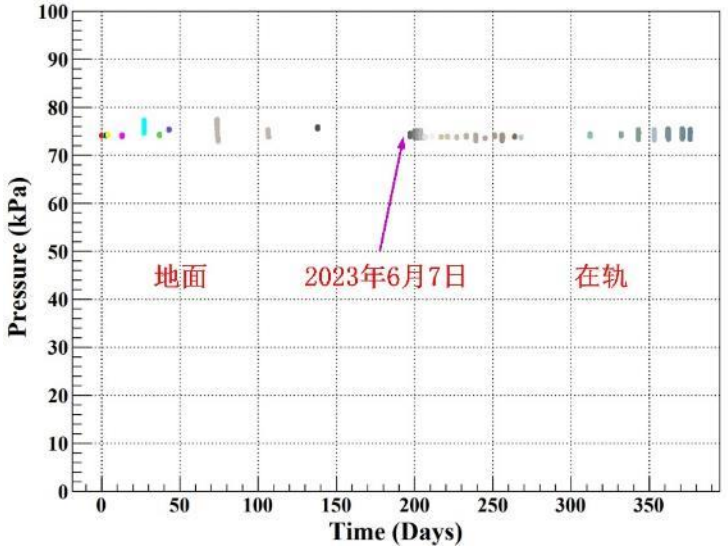

Gas pressure monitoring

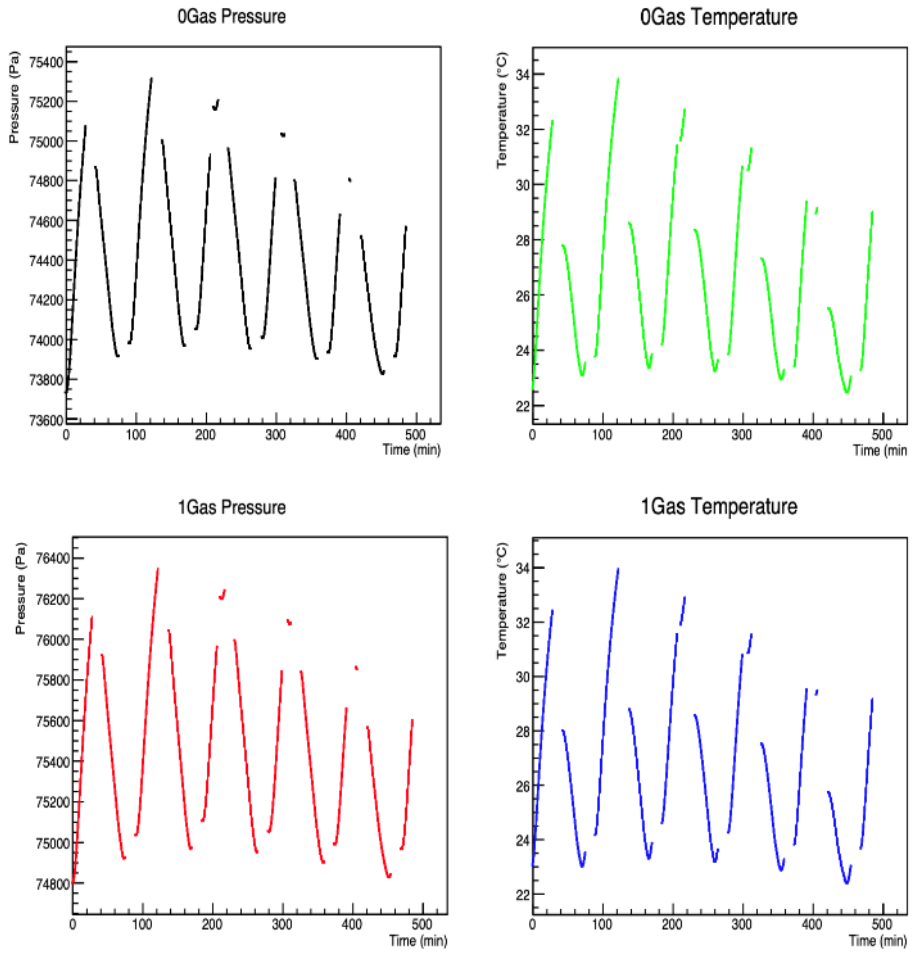

Gas pressure and temperature vary with the orbit

Status of CXPD payload

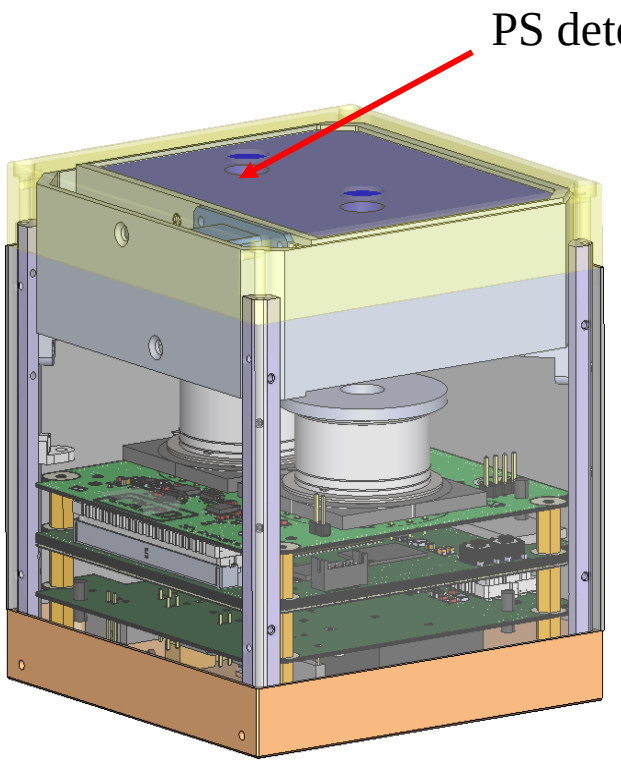

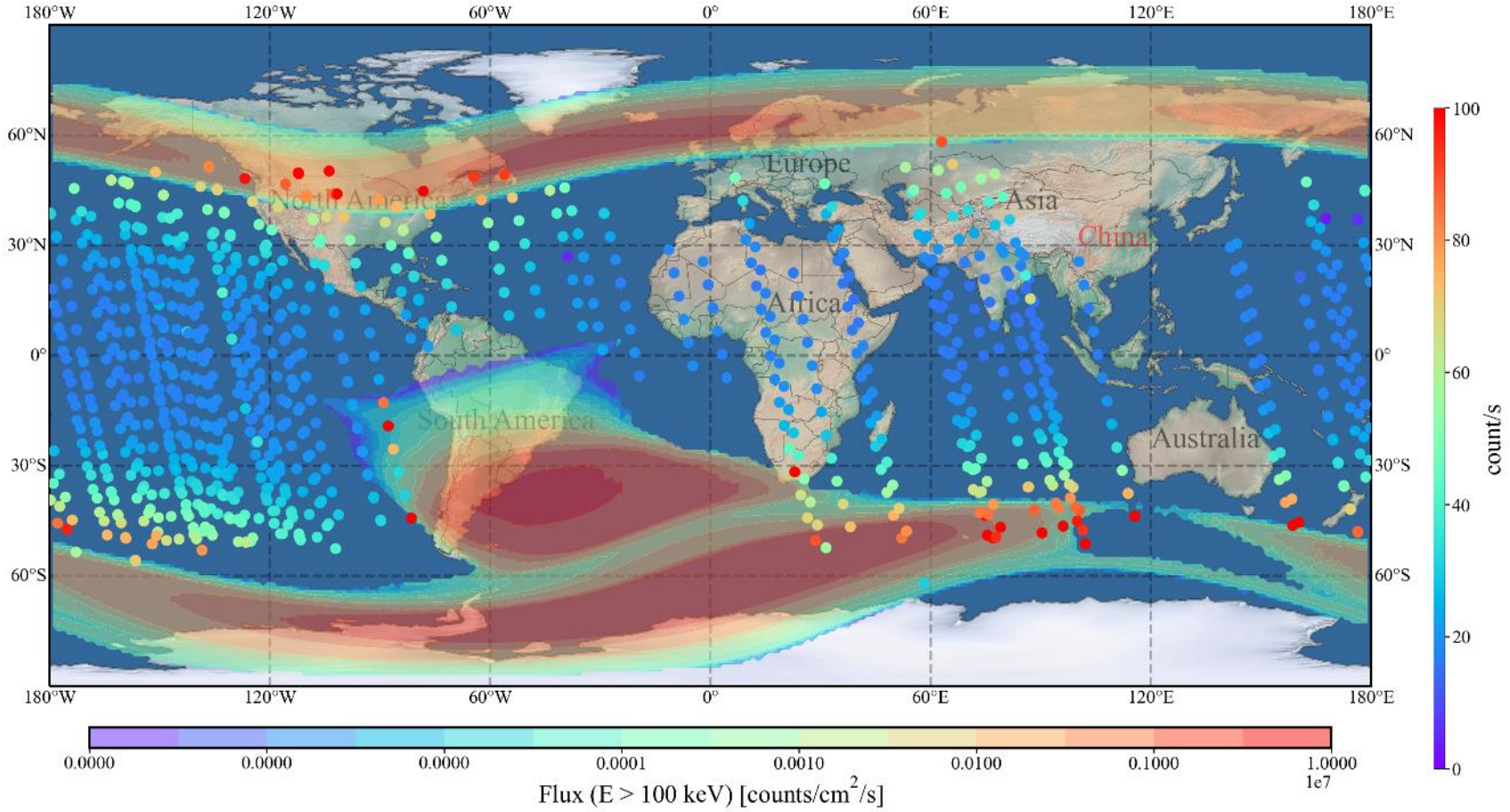

Particle background detect by PS detector

Status of CXPD payload

高压电源电压

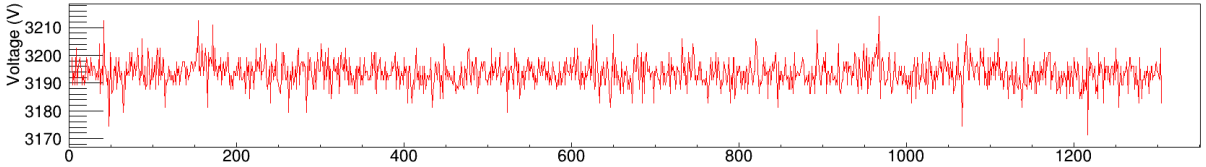

高压电源电流

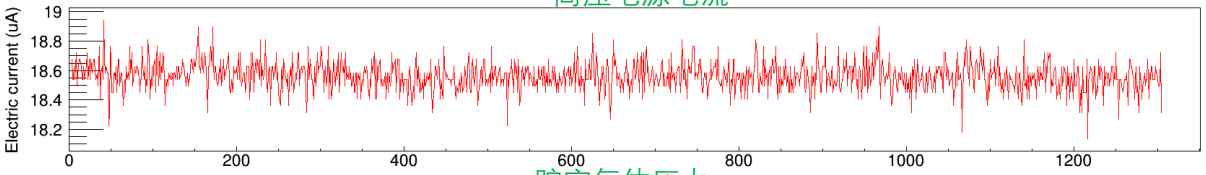

腔室气体压力

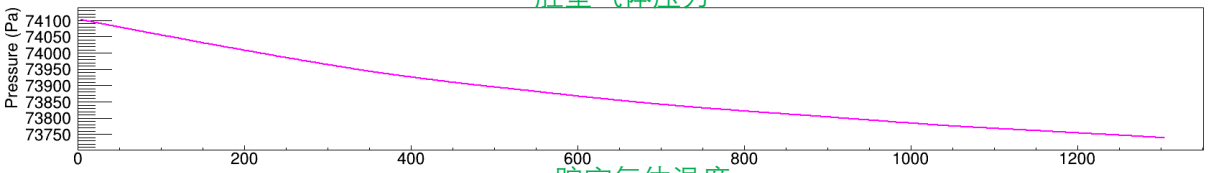

腔室气体温度

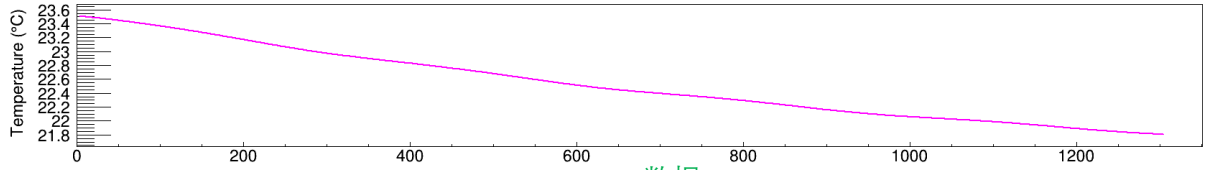

GMCP 数据

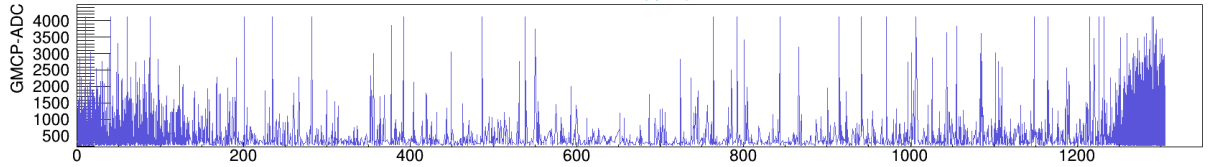

Topmetal 数据

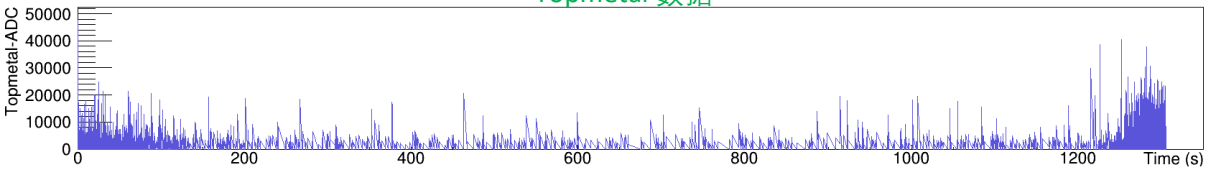

SiPM 数据

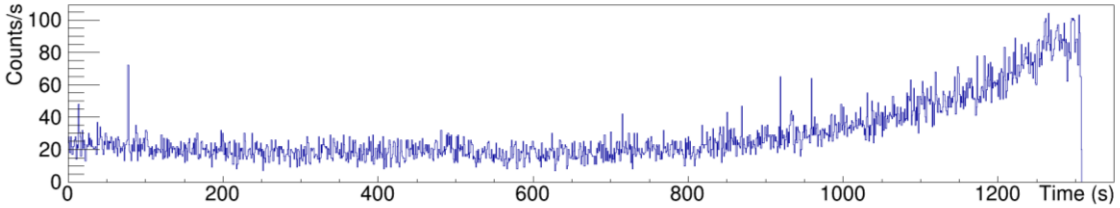

偏振探测器测量的径迹

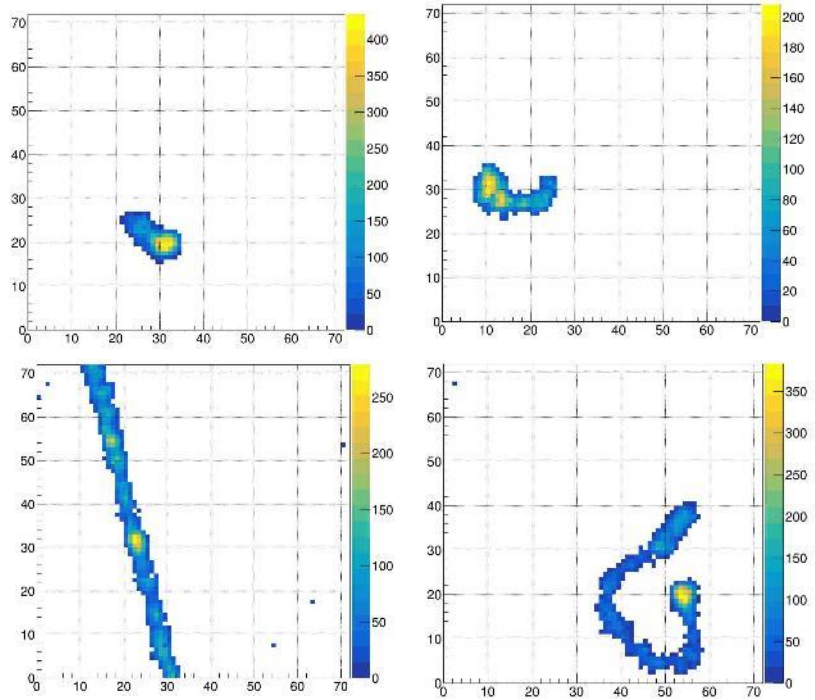

CXPD载荷的所有数据正常，工作良好，完成了空间X射线偏振测量的技术验证。

High Energy Cosmic Radiation Detection (HERD)

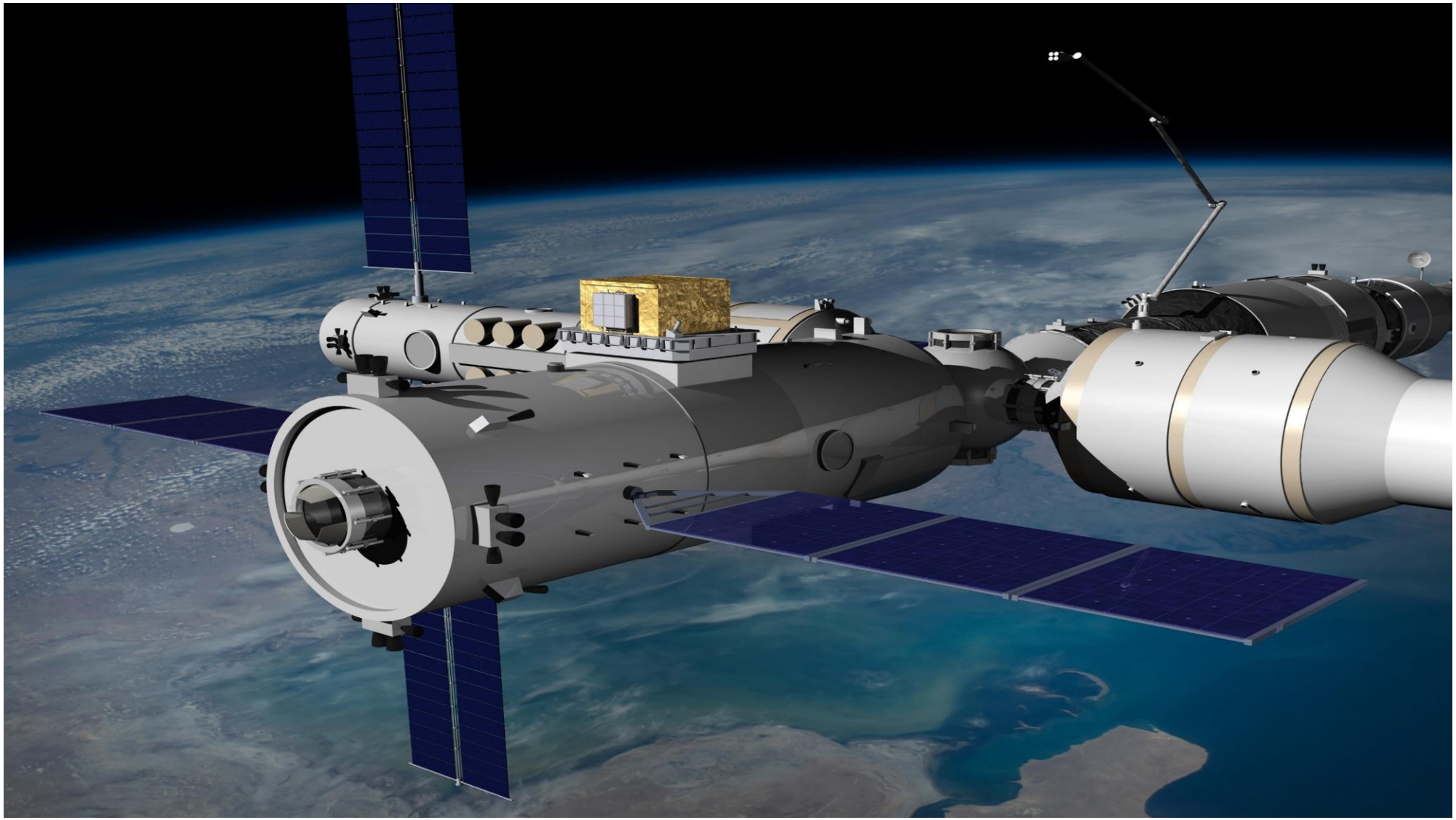

Energy Calibration for High-Energy Particles

- Current accelerator-based energy calibration techniques are limited to energies up to 400 GeV
- What alternative methods are available for energy calibration in the high-energy region (>TeV)?

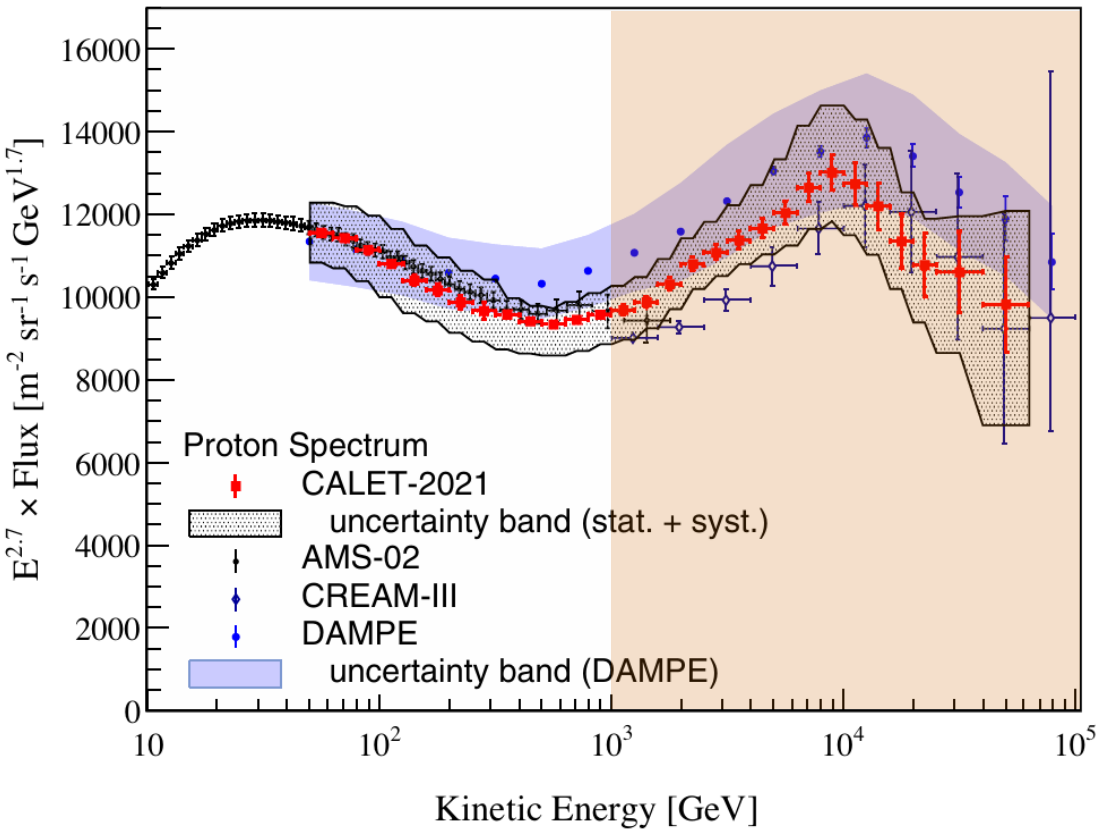

O. Adriani et al., Phys. Rev. Lett. 2022

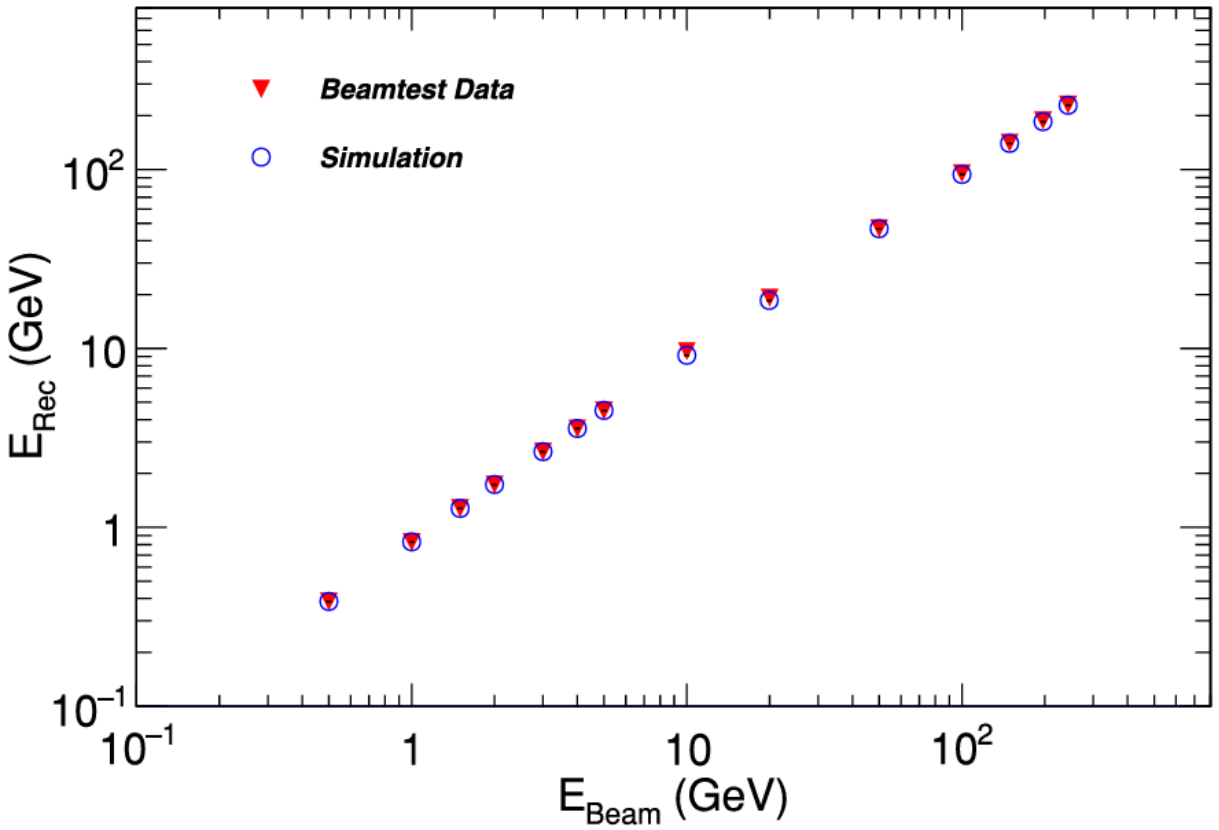

J. Chang et al., Astropart. Phys. 2017

Transition Radiation (TR) and Energy Calibration

- TR is generated when extremely relativistic charged particles pass through the interface between media with different dielectric constants

$$\left(\frac{d^2W_{TR}}{d\omega d\theta}\right)_{\text{stack}} = \frac{2\alpha\theta^3 Z^2}{\pi}\left(\frac{1}{\gamma^{-2}+\theta^2+\xi_1^2}-\frac{1}{\gamma^{-2}+\theta^2+\xi_2^2}\right)^2 \times 4\sin^2\left(\frac{l_1}{z_1}\right) \times \frac{\sin^2[N(l_1/z_1+l_2/z_2)]}{\sin^2[l_1/z_1+l_2/z_2]}$$

- The TR intensity is proportional to γ: $W_{\text{TR}} = \frac{\alpha Z^2}{3}\frac{(\omega_1-\omega_2)^2}{\omega_1+\omega_2}\gamma$
- Different particles exhibit the same TR intensity

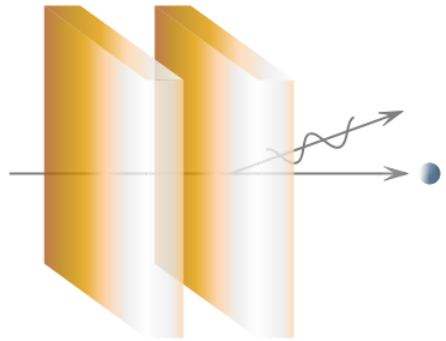

TR generation

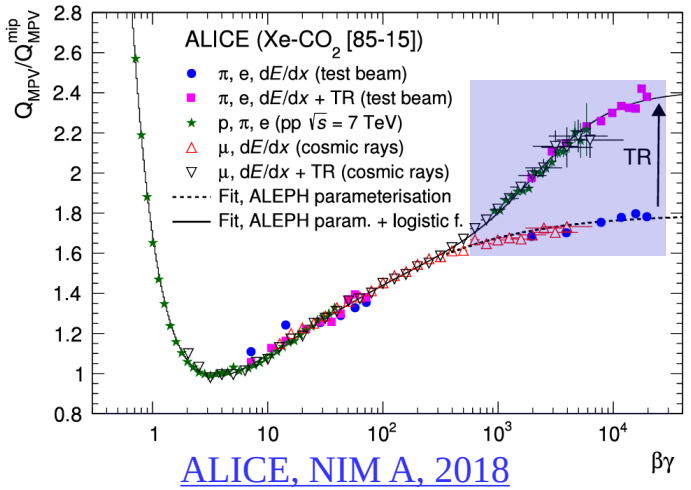

ALICE, NIM A, 2018

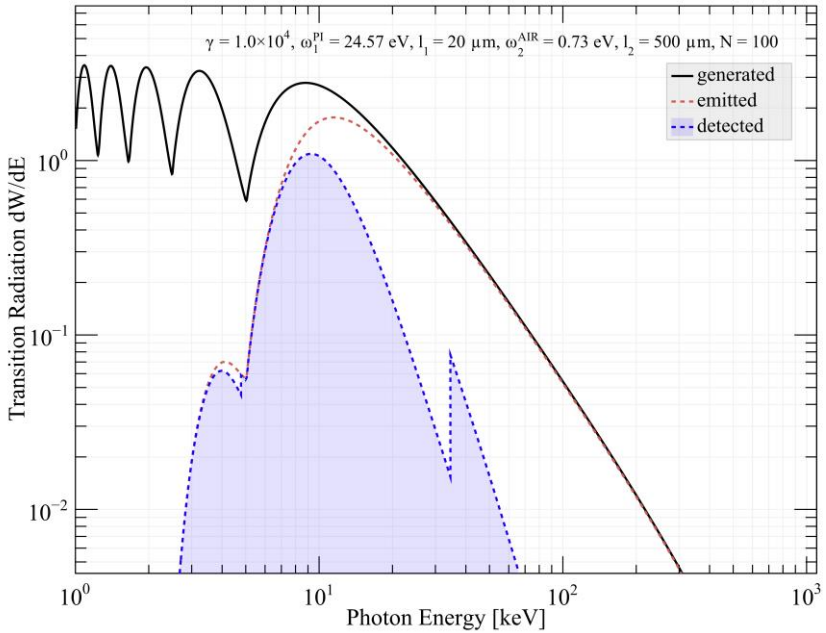

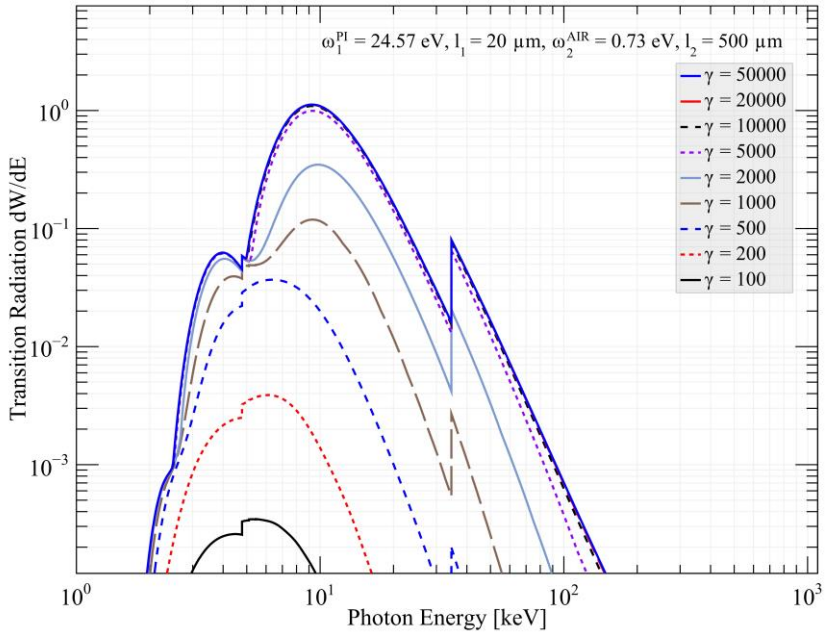

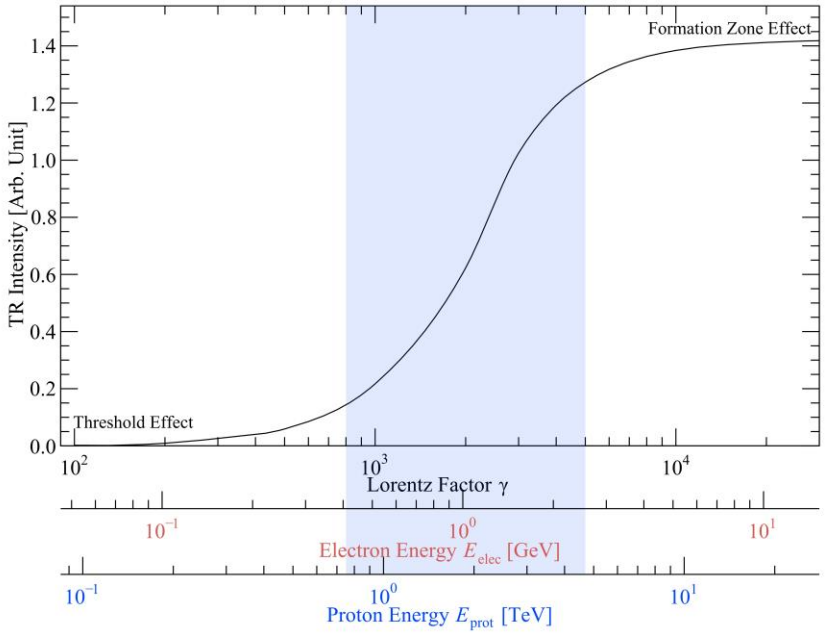

Overview of HERD/TRD Structure

- **The TRD provides in-orbit TeV energy calibration**
  - **The statistical TR response measured by TRD**
  - **Calibrated energy above 1TeV**
  - **Expected performance: better than 10% @ 2 TeV**

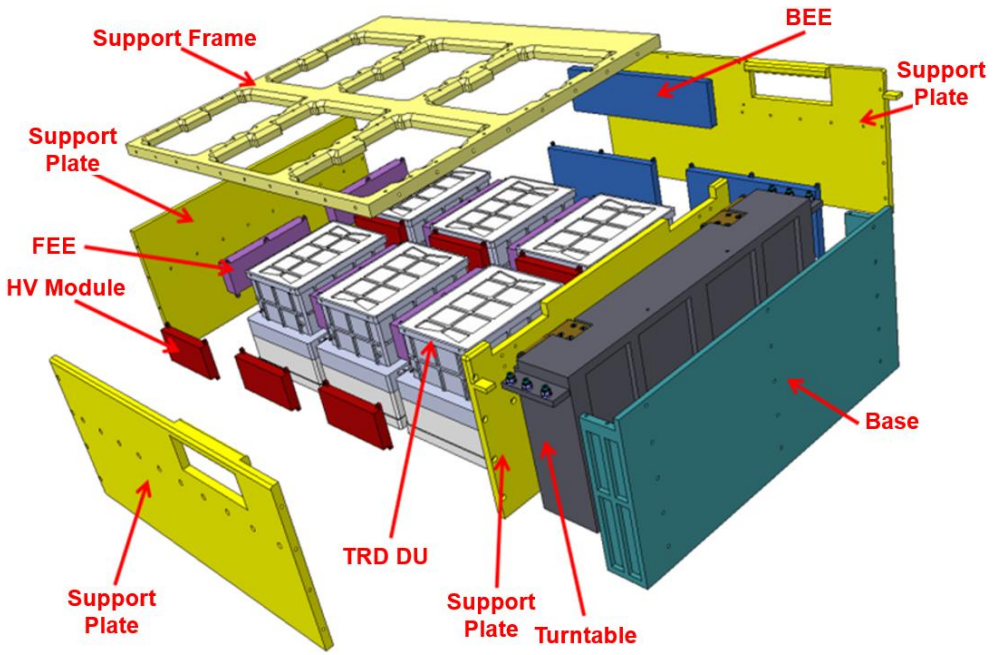

Schematic of HERD/TRD

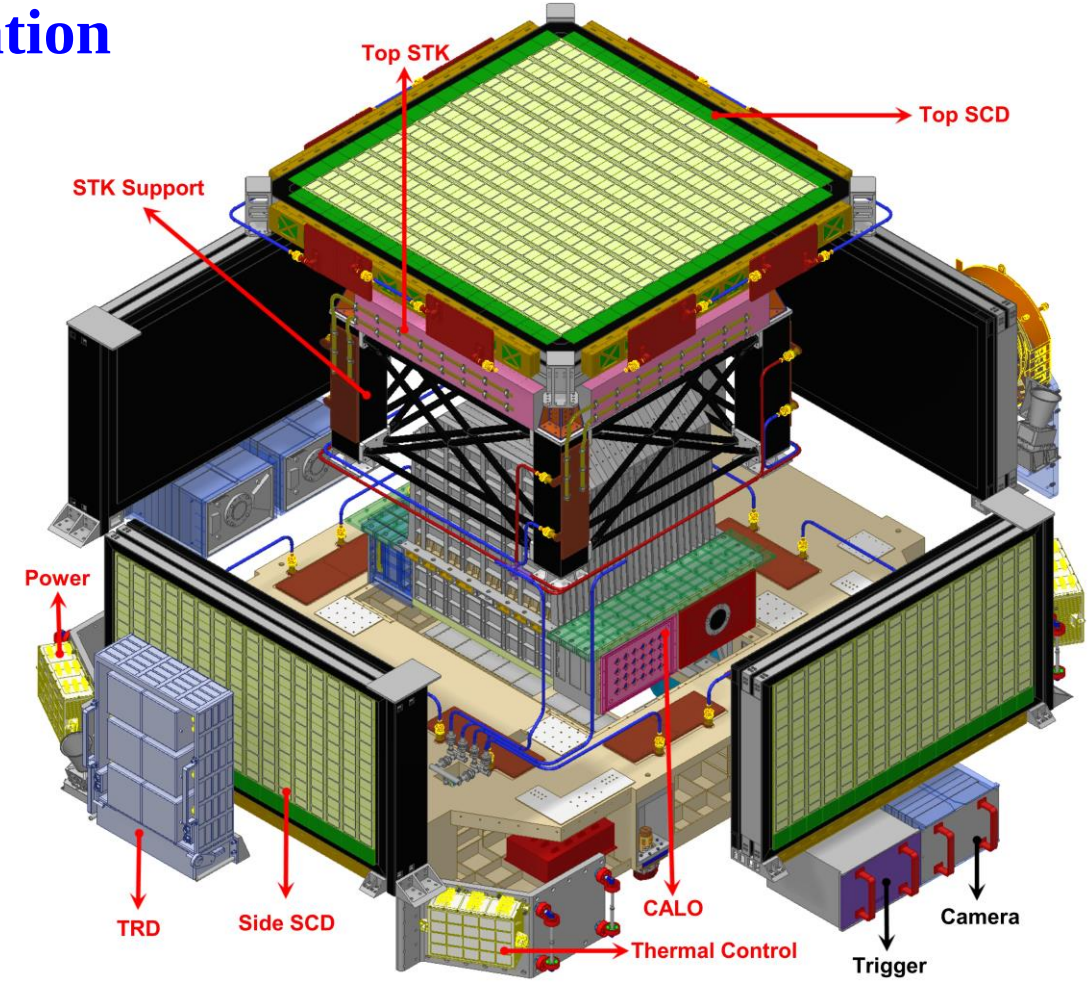

Schematic of HERD Payload

Side-on TRD detector unit

- Radiator: TR-photon generation
- Membrane: separated gas
- Frame: installation and fixation
- Cage: drift region electric field
- Cathode: negative high voltage
- THGEM: electron multiplication
- Anode: electron collection
- J30J: signal extraction
- HV Module: provides high voltage
- Electronics (FEE + BEE): data readout

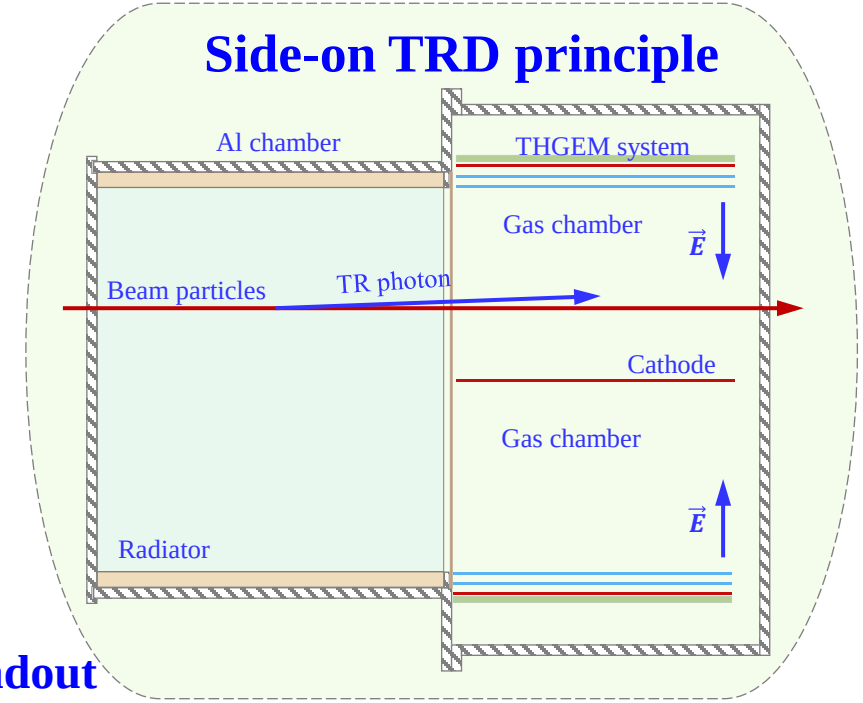

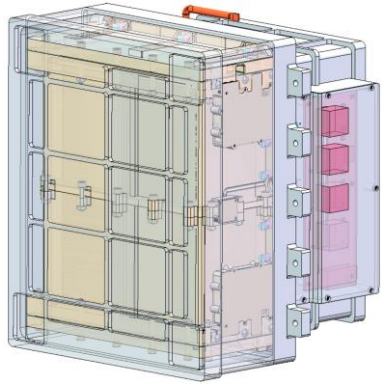

detector unit

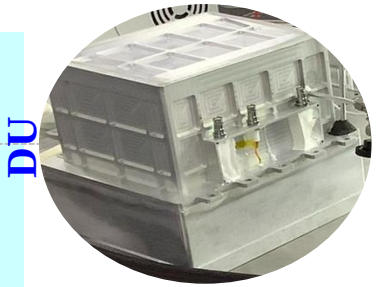

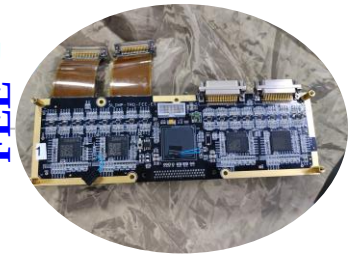

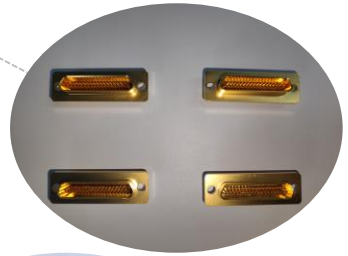

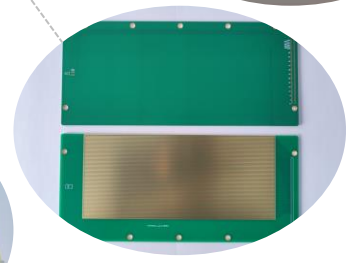

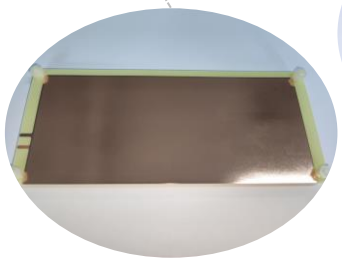

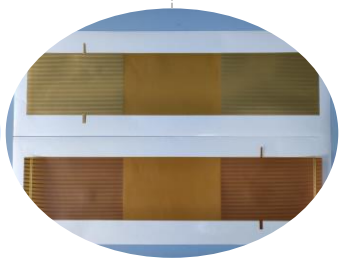

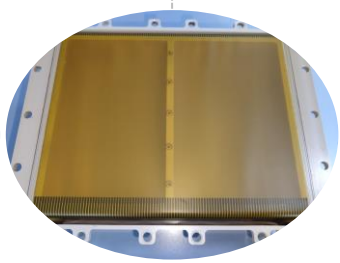

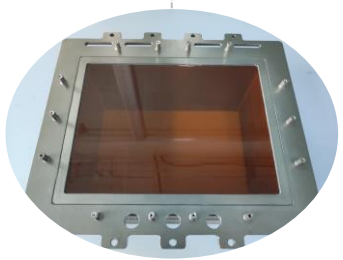

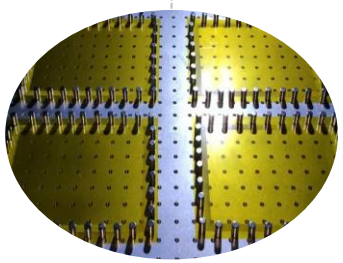

TRD Prototype Development

— 2018	BT2018@CERN	BT2019@IHEP	BT2019@DESY	BT2022@CERN	2023.02	BT2023@CERN
Proposed	Principle Prototype	TR-photon yield	Response curve	Fully Sealed Prototype	Mechanical Testing	Final prototype

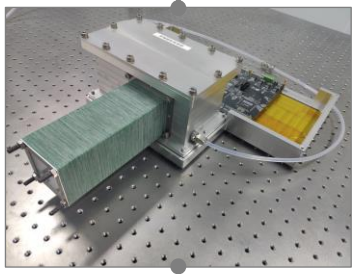

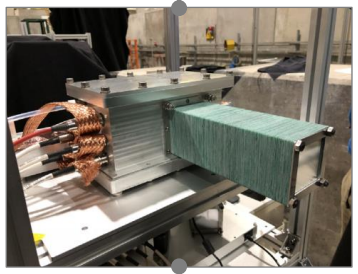

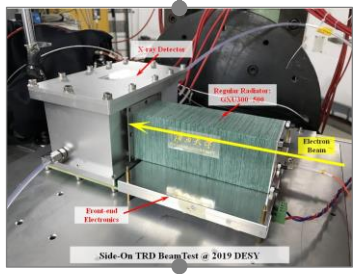

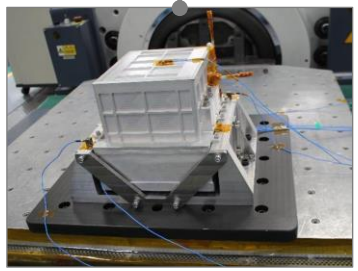

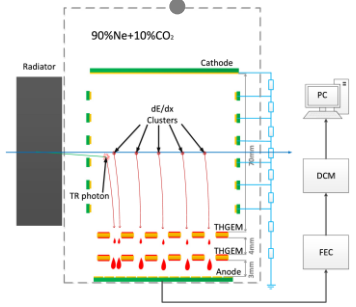

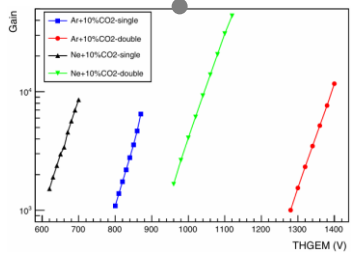

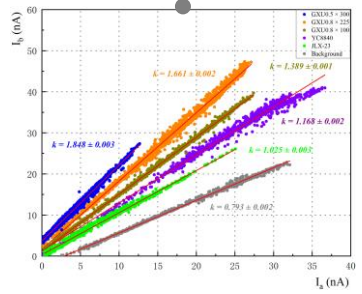

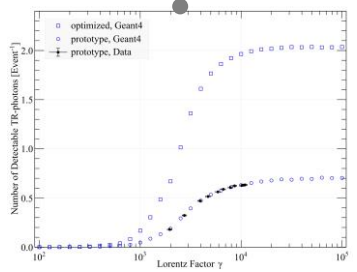

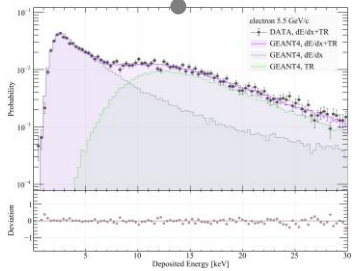

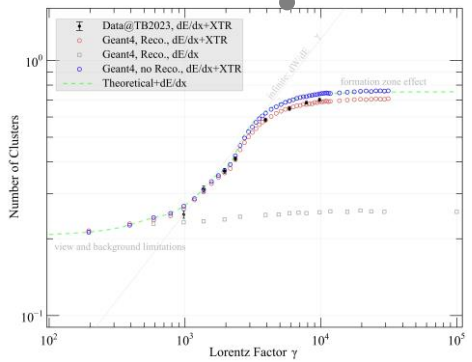

- B. Huang et al., NIM A 2020
- X. Liu et al., RDTM 2020
- J. Gu et al., JINST 2022
- C. Dai et al., JINST 2023
- C. Dai et al., ICRC 2023

The experiment is consistent with theory and simulation.

TeV Energy-Calibration Precision

- **TRD energy resolution:**
  - $\Delta E/E = \Delta\Re(E)/[E\Re'(E)]$, (S. Wakely, Astropart. Phys. 2002)
- **TRD resolution depend on the TR intensity**
  - **Energy range: 0.8 to 3.2 TeV**
  - **Precision: 10% @ 3 months**

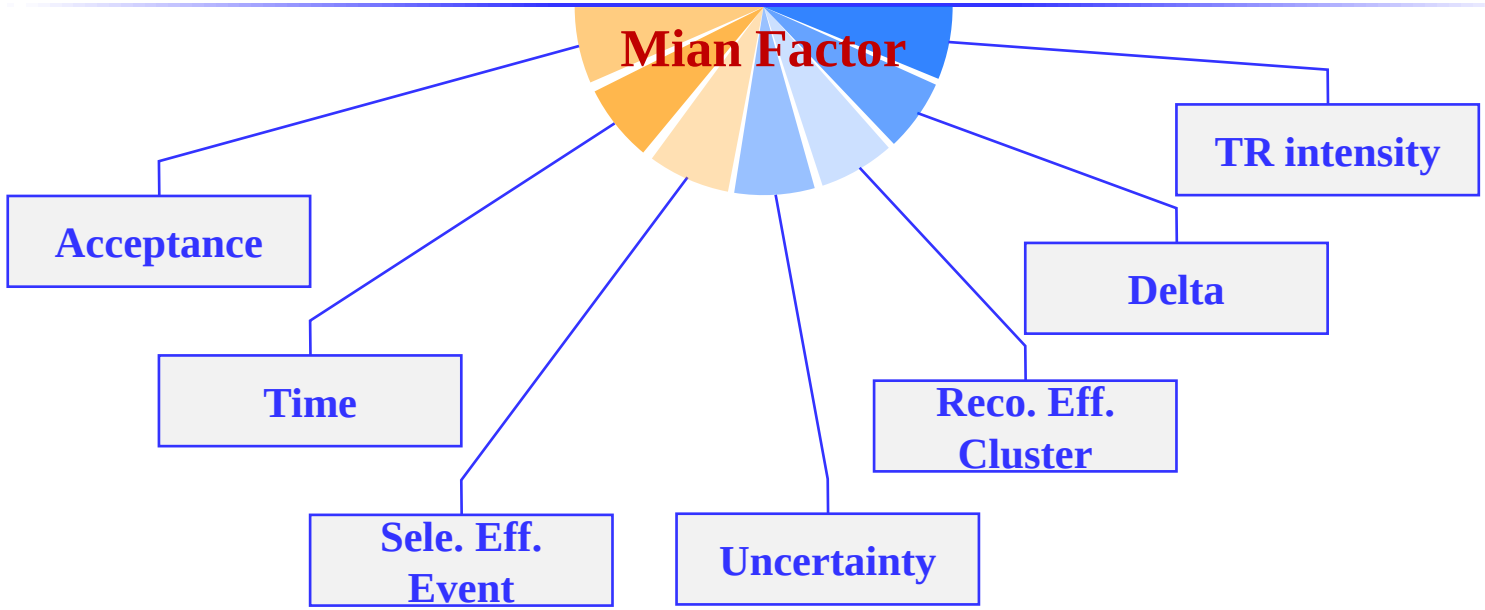

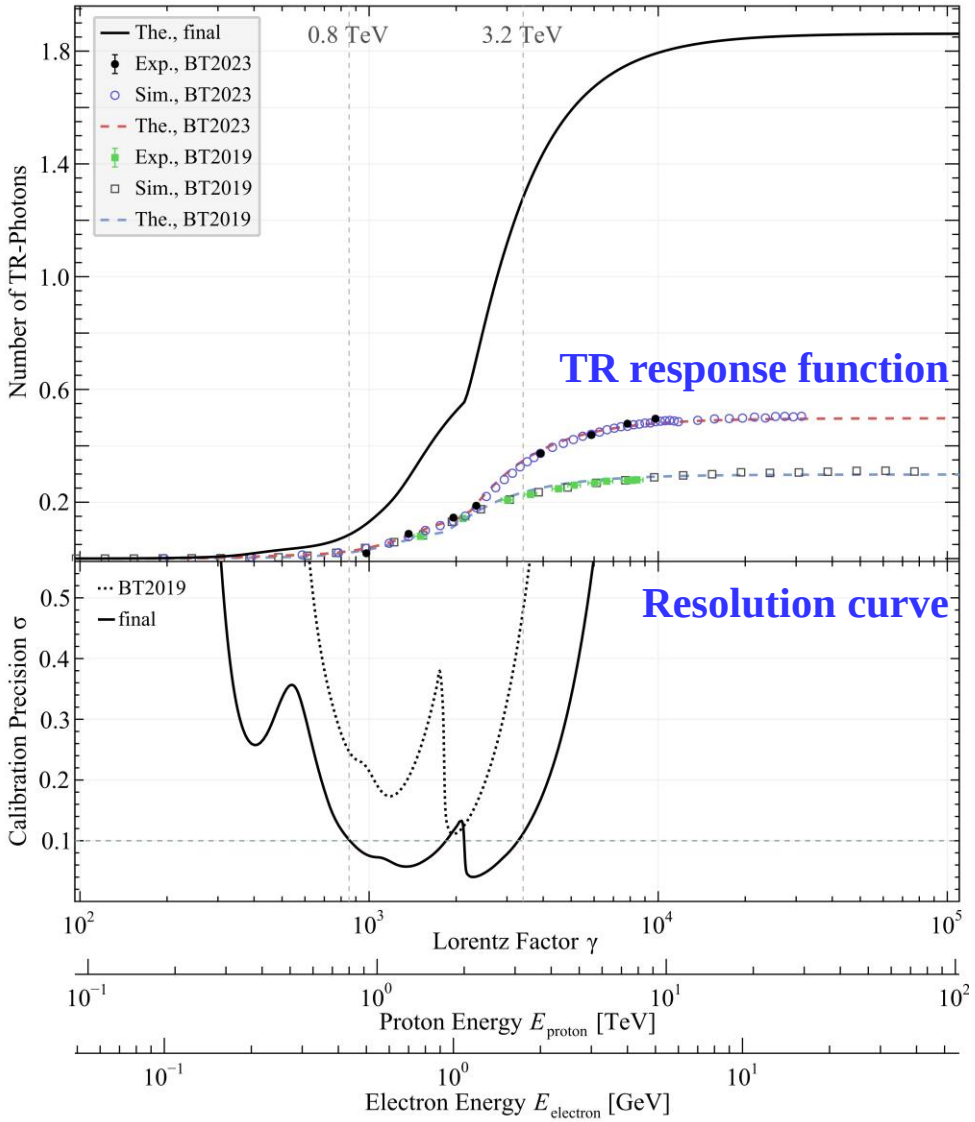

Thanks!